ISSN 0736-5306

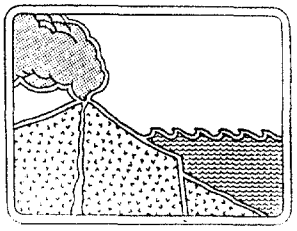

SCIENCE OF TSUNAMI HAZARDS

The International Journal of The Tsunami Society

Volume 13 Number 1 1995

OBJECTIVE: **The Tsunami Society** publishes this journal to increase and disseminate knowledge about tsunamis and their hazards.

DISCLAIMER: Although these articles have been technically reviewed by peers, **The Tsunami Society** is not responsible for the veracity of any statement, opinion or consequences.

Submit manuscripts of articles, notes or letters to the Editor. If an article is accepted for publication the author(s) must submit a camera ready manuscript in the journal format. A voluntary $50.00 page charge ($35.00 for Tsunami Society Members) will include 50 reprints.

SUBSCRIPTION INFORMATION: Price per copy $20.00 USA

ISSN 0736-5306

Published by **The Tsunami Society** in Honolulu, Hawaii, USA

LONG WAVES IN TWO-LAYERS : GOVERNING EQUATIONS AND NUMERICAL MODEL

Fumihiko IMAMURA
Disaster Control Research Center, Tohoku University
Aoba, Sendai 980-77, Japan

and

Md.Monzur Alam IMTEAZ
Dept. of Civil Engineering, Saitama University
255, Shimo-Okubo, Urawa city 338, Japan

ABSTRACT

Governing equations including full non-linearity are derived from the Euler equations of mass and momentum continuities assuming a long wave approximation, negligible friction and interfacial mixing. The linearized equations for two-layers are analytically solved using the Fourier transform. A numerical model is developed using the staggered leap-frog scheme for computation of water level and discharge in one dimensional propagation. Results of the numerical model are verified by comparing with the analytical solution for different boundary conditions. Good agreements between analytical and numerical model are observed for the boundary conditions using the characteristics method to estimate the representative celerity at the previous time step. The stability condition is discussed and it was found that CFL stability condition considering fixed interface and top surface wave celerities as the physical celerity is not directly applicable. A modified stability condition taking the maximum celerity among them, $\Delta t \leq \Delta x / \max(c_1, c_2)$, is proposed. The properties of two-layers long waves is discussed through numerical simulations with different values of α (ratio of density of fluid in an upper layer to a lower one) and β (ratio of water depth in a lower layer to an upper one). It is suggested that as α increases amplification of top surface decreases and vice versa. Again as β increases amplification of a top surface also increases and vice versa.

1. INTRODUCTION

Tsunamis are generated due to disturbances of a free surface caused by not only seismic fault motion but also landslide, volcanic eruptions and so on. Since most of them are caused by earthquakes and a tsunami is categorized into a long wave, the long wave theory in one layer model as the governing equations for analytical and numerical models has been applied. However, as we find in many references **[HAMPTOM(1972) ; PARKER (1982); HARBITZ(1991); JIANG AND LEBLOND(1992)]**, two-layers long waves or flows (surface wave and mudslide as example) are also found and reported in the case of underwater landslides generating tsunamis. Therefore, two- or multi-layers long waves model fully including an interaction between each layer instead of the previous one-layer model is required to reproduce an excitation of a top surface on an interface.

Two-layers flow with different density is related to many environmental phenomena as well. Thermally driven exchange flows through channel to oceanic currents such as the flow through the Strait of Gibraltar is an example of two-layers flow. Also salt water intrusion in estuaries, spillage of the oil on the sea surface, spreading of dense contaminated water, sediment laden discharges into lakes, generation of lee waves behind a mountain range and tidal flows over sills of the ocean are also examples.

This type of flow is often termed as a gravity current. Due to the extra weight of the denser fluid, a larger piezometric surface exists inside the current than in the fluid ahead, and this provides the motive force. When denser fluid is introduced into a less dense environment, this dense fluid spreads under the action of buoyancy force and often travels down an incline. **SIMPSON (1982)** has provided extensive review on hydrodynamics of various gravity currents and powder snow avalanches. The difference in density that provides the motive force may be due to dissolved substances or temperature differences, or due to suspended material. The internal hydraulics of a single layer, either beneath or above a stagnant or passive layer, is discussed in standard references **[cf. PRANDTL (1952) ; TURNER (1973)]**, and the study of a two-layers flow in which both layers interact and play a significant role in the establishment of control of the flow is described.

In the past years a number of analytical and experimental studies were carried out on two layer flow. And some numerical models on unsteady gravity currents are also proposed[e.g. **AKIYAMA., WAN. & URA (1990); JIANG AND LEBLOND (1992); KRANENBURG. (1993)**]. Although almost all of them compared their numerical results with experimental and observed results, there are still some questions regarding their reliability in terms of accuracy. The effect of the mixing or entrainment process at a front or an interface is very important **[ELLISON AND TURNER (1959)]** but the physical model of the mixing has not been successfully developed. Therefore accuracy and stability of the numerical models are not well discussed. In the present paper, we focus on the governing equations and numerical modeling for two-layers excluding the mixing process. And we study the reliability and accuracy of the proposed numerical model through the comparison with the analytical solution under simplified conditions. The properties of two-layers long waves and excitation on the free surface due to the interaction of two-la yers waves are discussed.

2. THEORETICAL CONSIDERATION

Governing Equations :

A mathematical model for two-layers flow in a wide channel with non-horizontal bottom was studied assuming a hydrostatic pressure distribution, negligible friction and negligible interfacial mixing which are , however, important in an underwater landslides. Also uniform density and

velocity distributions in each layer were assumed. Considering the two-dimensional case, Fig.1, Euler equations of mass and momentum continuities are integrated in each layer, with the kinetic and dynamic conditions at the free surface and interface. The details of the derivation are described in **IMTEAZ(1993)** and in the Appendix.

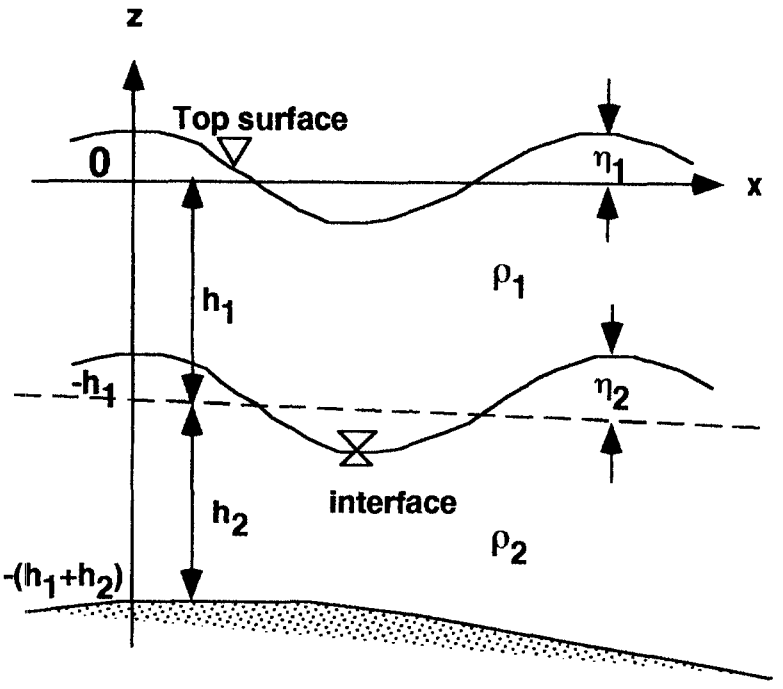

Figure 1 Definition sketch for two-layers profile.

Governing equations for an upper layer are given by

$$\frac{\partial(\eta_1-\eta_2)}{\partial t}+\frac{\partial M_1}{\partial x}=0 \qquad (1)$$

$$\frac{\partial M_1}{\partial t}+\frac{\partial\left(\frac{M_1^2}{D_1}\right)}{\partial x}+gD_1\frac{\partial \eta_1}{\partial x}=0 \qquad (2)$$

and those for a lower layer are

$$\frac{\partial \eta_2}{\partial t}+\frac{\partial M_2}{\partial x}=0 \qquad (3)$$

$$\frac{\partial M_2}{\partial t}+\frac{\partial\left(\frac{M_2^2}{D_2}\right)}{\partial x}+gD_2\left\{\alpha\left(\frac{\partial \eta_1}{\partial x}+\frac{\partial h_1}{\partial x}-\frac{\partial \eta_2}{\partial x}\right)+\frac{\partial \eta_2}{\partial x}-\frac{\partial h_1}{\partial x}\right\}=0 \qquad (4)$$

Where η is the water surface elevation, $D=h+\eta$ the total depth , h the still water depth, M the discharge, ρ the density of fluid, $\alpha=\rho_1/\rho_2$, and subscripts 1 and 2 indicate the upper and lower layer respectively.

Linearized Equation :

Generally it is difficult to handle the derived momentum equations, because some non-linear terms are included in the momentum equations. As long as the amplitude of waves are small compared with the still water depth, such non-linear terms is neglected. Then, the linear governing equations can be used in the case of small amplitude waves.

Linearized equations for an upper layer are obtained as follows:

$$\frac{\partial(\eta_1-\eta_2)}{\partial t}+\frac{\partial M_1}{\partial x}=0 \qquad (5)$$

$$\frac{\partial M_1}{\partial t}+gh_1\frac{\partial \eta_1}{\partial x}=0 \qquad (6)$$

and for a lower layer:

$$\frac{\partial \eta_2}{\partial t}+\frac{\partial M_2}{\partial x}=0 \qquad (7)$$

$$\frac{\partial M_2}{\partial t}+gh_2\left\{\alpha\left(\frac{\partial \eta_1}{\partial x}+\frac{\partial h_1}{\partial x}-\frac{\partial \eta_2}{\partial x}\right)+\frac{\partial \eta_2}{\partial x}-\frac{\partial h_1}{\partial x}\right\}+g\eta_2(\alpha-1)\frac{\partial h_1}{\partial x}=0 \qquad (8)$$

The effects of a lower layer on an upper one are found in the mass conservation equation in a lower layer, and those of an upper layer on a lower one are in the momentum equation in a lower layer. The both effects of interaction between the two layers play an important role on wave propagation and the amplification of a top surface or an interface.

3. ANALYTICAL SOLUTION

The solution of the non-linear governing equations can not be obtained analytically without some assumption or simplification. So linearized governing equations assuming a flat bottom have been solved analytically to test the validity of the numerical model. By simple differential operation and substitution, four linearized equations are transformed into two equations. Upper and lower layer equations are respectively obtained as

$$\frac{\partial^2 \eta_1}{\partial t^2}-gh_1(1+\alpha\beta)\frac{\partial^2 \eta_1}{\partial x^2}-gh_2(1-\alpha)\frac{\partial^2 \eta_2}{\partial x^2}=0 \qquad (9)$$

and

$$(1+\alpha\beta)\frac{\partial^2 \eta_2}{\partial t^2}-gh_2(1-\alpha)\frac{\partial^2 \eta_2}{\partial x^2}-\alpha\beta\frac{\partial^2 \eta_1}{\partial t^2}=0 \qquad (10)$$

where β is h_2/h_1. The last terms as an external force in the above two equations are added into the simple wave equation.

Let us derive the solution using the Fourier transform. If we consider the progressive wave at the interface, η_2 can be expressed by,

$$\eta_2 = \int_{-\infty}^{+\infty} \tilde{\eta}(k) e^{ik(x-c_2 t)} dk \qquad (11)$$

where $\tilde{\eta}$ is the amplitude of the Fourier series for the initial condition and $c_2 = \sqrt{gh_2(1-\alpha)/(1+\alpha\beta)}$, and k is the wave number. Then, the water surface in an upper layer can be assumed as,

$$\eta_1 = \int_{-\infty}^{+\infty} a(k,t)\tilde{\eta}(k) e^{ik(x-c_1 t)} dk \qquad (12)$$

where $c_1 = \sqrt{gh_1(1+\alpha\beta)}$.

and a(k,t) is a function of time and wave number to be solved. It is a reasonable assumption for initial boundary condition that at t=0, $\eta_1 = 0$ and $\partial\eta_1/\partial t = \partial\eta_2/\partial t$. Initial and boundary conditions are illustrated in Fig.2.

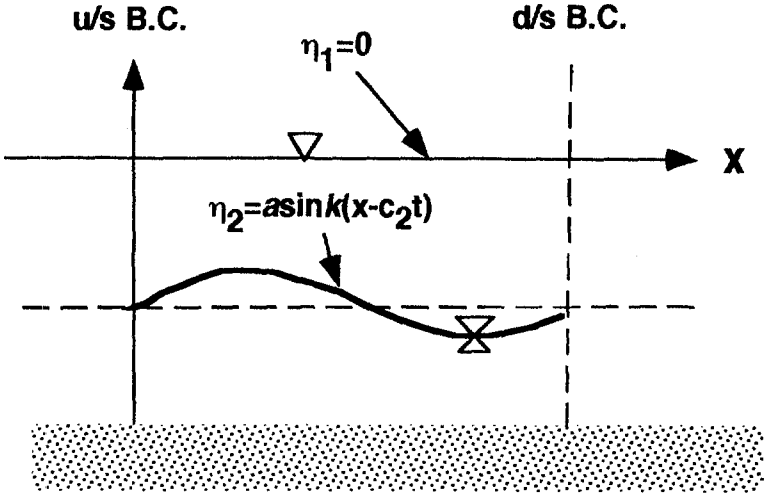

Figure 2 Sketch of initial and boundary (periodic) conditions.

Substituting Eqs.(11) and (12) into Eq.(9) we get the following ordinary differential equation for a:

$$\int_{-\infty}^{+\infty}\left[\frac{d^2a}{dt^2} - 2ikc_1\frac{da}{dt} + gh_2k^2 a e^{ik(c_1-c_2)t}\right]\tilde{\eta}e^{ik(x-c_1 t)}dk = 0 \qquad (13)$$

Integration of Eq.(13) with respect to time with the initial condition that $\partial\eta_1/\partial t = \partial\eta_2/\partial t$ yields,

$$\frac{da}{dt} = ikac_1 - ikc_2 \qquad (14)$$

In addition, using the first initial condition that at t=0, a=0, we can obtain the solution of a,

$$a = -\frac{gh_2(1-\alpha)}{c_1 - c_2}\left[\frac{e^{ik(c_1-c_2)t}}{c_1+c_2} - \frac{1}{2c_1}\right] + \frac{c_2}{2c_1}\left[\frac{gh_2 e^{ik(c_1-c_2)t}}{2c_1(c_1+c_2)} - \frac{c_2}{2c_1}\right] e^{2ikc_1 t} \qquad (15)$$

Finally, substitution of Eq.(15) into Eq.(12) yields the solution for the wave profile in the upper layer as follows :

$$\begin{aligned}\eta_1 = &-\left[\frac{gh_2(1-\alpha)}{c_1^2 - c_2^2}\right]\int_{-\infty}^{+\infty}\tilde{\eta}e^{ik(x-c_2t)}dk + \left[\frac{gh_2(1-\alpha)}{2c_1(c_1-c_2)} + \frac{c_2}{2c_1}\right]\int_{-\infty}^{+\infty}\tilde{\eta}e^{ik(x-c_1t)}dk \\ &+\left[\frac{gh_2(1-\alpha)}{2c_1(c_1+c_2)} - \frac{c_2}{2c_1}\right]\int_{-\infty}^{+\infty}\tilde{\eta}e^{ik(x+c_1t)}dk\end{aligned} \qquad (16)$$

Solution for η_1 consists of three wave components; two progressive waves and one reflective wave. One of the progressive waves has one celerity, c_1 , and the other has another one, c_2. The reflective wave component has celerity c_1. To get a clear idea of the analytical solution, Eq.(16), we calculate wave profiles with three components of top surface, resultant wave profile for a top surface, and wave shape for an interface shown in Fig.3. It is indicated that in the case of α=0.01 and β=1.0, the two progressive waves are much larger than the reflective wave. But two progressive components have opposite in sign, so the resultant of them become smaller and comparable with the reflective one.

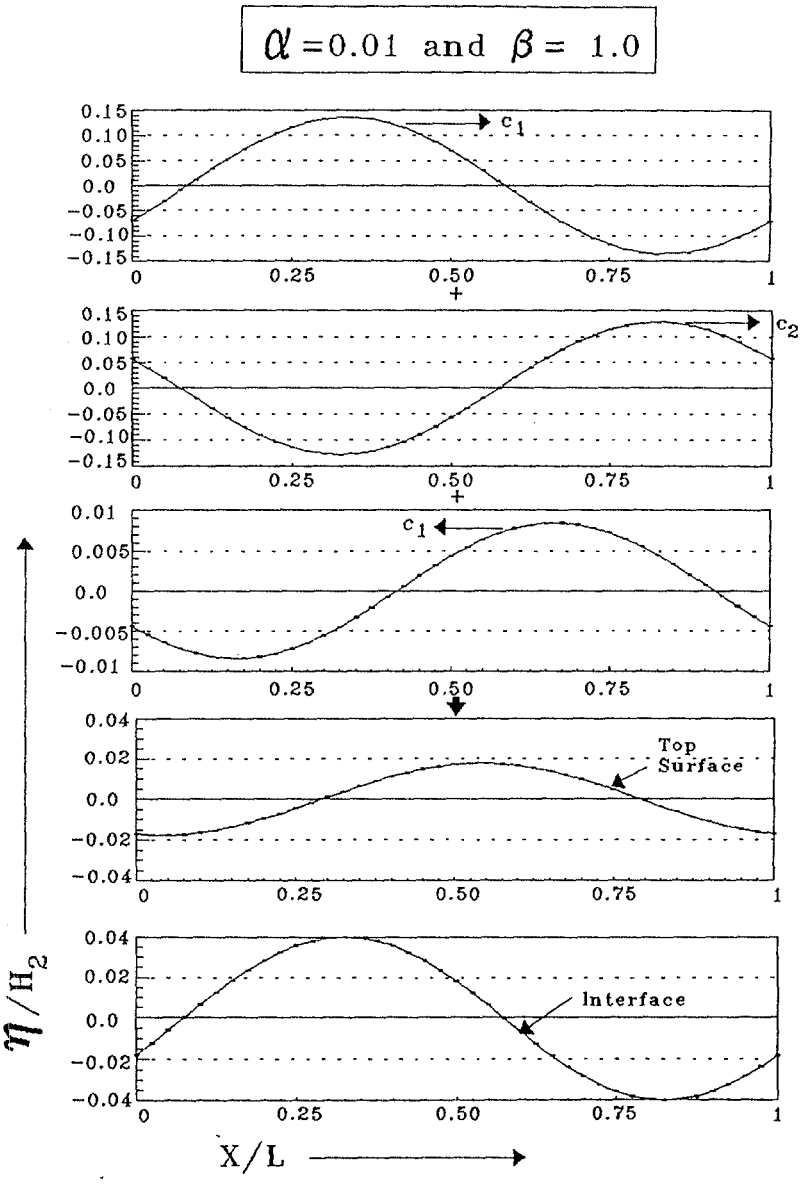

Figure 3 Resultant of analytical solution of top surface and interface (two lower) consisting three wave components (three upper).

4. NUMERICAL MODEL

Numerical Scheme

The staggered leap-frog scheme **[IMAMURA (1995)]**has been used to solve the governing equations for long waves numerically. This scheme is one of explicit central difference schemes with the truncation error of second order. The staggered scheme considers that the computation point for one variable,η, does not coincides with the computation point for other variable, M. There are half step differences, $1/2\Delta t$ and $1/2\Delta x$ between computation points of two variables as shown in Fig.4. Thus one variable,η, is placed at the middle of $\Delta t\Delta x$ rectangle, placing other

variables at the four corner of rectangle and vice versa. Using this scheme, the finite difference equations for the proposed governing equations are obtained as follows:

for an upper layer,

$$\frac{\eta_{1_{i+\frac{1}{2}}}^{n+\frac{1}{2}} - \eta_{1_{i+\frac{1}{2}}}^{n-\frac{1}{2}} - \eta_{2_{i+\frac{1}{2}}}^{n+\frac{1}{2}} + \eta_{2_{i+\frac{1}{2}}}^{n-\frac{1}{2}}}{\Delta t} + \frac{M_1{}_{i+1}^{n} - M_1{}_{i-1}^{n}}{\Delta x} = 0$$

$$\frac{M_1{}_{i}^{n+1} - M_1{}_{i}^{n}}{\Delta t} + g\frac{h_{1_{i+\frac{1}{2}}} + h_{1_{i-\frac{1}{2}}}}{2}\frac{\eta_{1_{i+\frac{1}{2}}}^{n+\frac{1}{2}} - \eta_{1_{i-\frac{1}{2}}}^{n+\frac{1}{2}}}{\Delta x} = 0 \qquad (17)$$

and for a lower one,

$$\frac{\eta_{2_{i+\frac{1}{2}}}^{n+\frac{1}{2}} - \eta_{2_{i+\frac{1}{2}}}^{n-\frac{1}{2}}}{\Delta t} + \frac{M_2{}_{i+1}^{n} - M_2{}_{i-1}^{n}}{\Delta x} = 0$$

$$\frac{M_{2i}^{n+1} - M_{2i}^{n}}{\Delta t} + g(\alpha - 1)\frac{\eta_{2_{i+\frac{1}{2}}}^{n+\frac{1}{2}} + \eta_{2_{i-\frac{1}{2}}}^{n+\frac{1}{2}}}{2}\frac{h_{2i+\frac{1}{2}} - h_{2i-\frac{1}{2}}}{\Delta x} \qquad (18)$$

$$+g\frac{h_{2_{i+\frac{1}{2}}} + h_{2_{i-\frac{1}{2}}}}{2}\left[\alpha\frac{\eta_{1_{i+\frac{1}{2}}}^{n+\frac{1}{2}} - \eta_{1_{i-\frac{1}{2}}}^{n+\frac{1}{2}}}{\Delta x} + (\alpha - 1)\frac{h_{1_{i+\frac{1}{2}}} - h_{1_{i-\frac{1}{2}}}}{\Delta x} + (1-\alpha)\frac{\eta_{2_{i+\frac{1}{2}}}^{n+\frac{1}{2}} - \eta_{2_{i-\frac{1}{2}}}^{n+\frac{1}{2}}}{\Delta x}\right] = 0$$

Where 'n' denotes the temporal grid points and 'i' denotes the spatial grid points as shown in Fig. 4. Δx and Δt are spatial grid spacing and time step respectively.

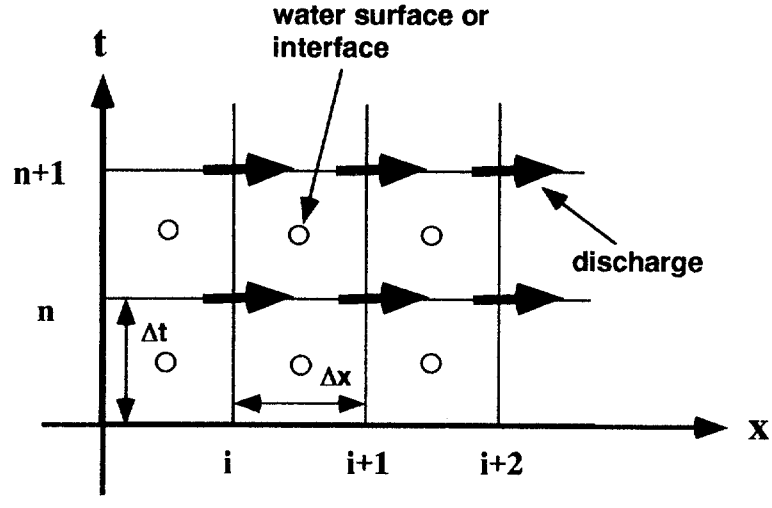

Figure 4 Points schematics of the staggered leap-frog scheme

In spatial direction, all of η_1, η_2 at step 'n+1/2' and all of M_1, M_2 at step 'n' are given as initial conditions. For all later time steps at left and right boundaries, all values of either discharge or water elevation would be calculated by a characteristic method etc., using the values of previous time step or estimated wave celerity. Later boundary conditions will be discussed in detail. By using the mass continuity equation for a lower layer, all η_2 at step 'n+3/2' are calculated and then all η_1 at step 'n+3/2' for an upper layer are calculated using latest values of η_2. Next, using the momentum equation for an upper and a lower layer, all values of M_2 at step 'n+1' are simultaneously calculated. Similarly, using new values of η_1, η_2, M_1 and M_2 as initial values for the next time step, the calculations proceeds in time direction up to desired step.

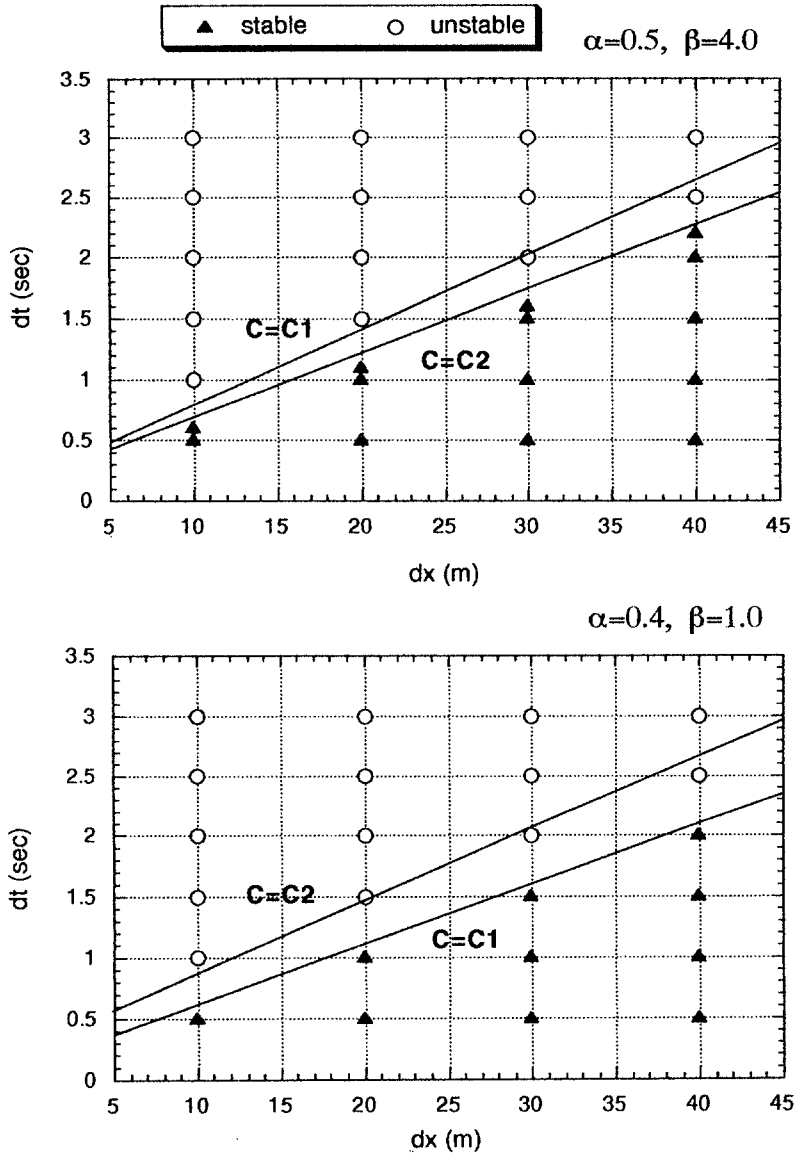

Figure 5 Critical condition of numerical stability. The border line of using C_1 in the upper figure corresponds to the critical condition obtained by the numerical simulation with different values of Δx and Δt, while that in the lower one is not.

Stability Condition

Due to the interactions between two layers, it is very difficult to derive a stability condition analytically using the Von Neumann method. The Courant-Friedrichs-Lewys (CFL) condition is normally applicable to the numerical scheme for wave propagation, however, in this case it is not directly applicable because the representative wave celerity is not specified. Two celerities for a progressive waves and one for reflected one exist. Therefore, stability is initially investigated for some arbitrary Δx and Δt. This result, shown in Fig.5, suggests that the model is stable up to a certain limit of $\Delta x/\Delta t$ and this limit varies with the variation of α and β as shown in Fig.5. In the cases with α=0.5 and β=4.0 , celerity of top surface calculated through analytical expression, c_2[$=\sqrt{gh_2(1-\alpha)/(1+\alpha\beta)}$], controls the stability criteria. But for the other case with α=0.4 and β=1.0 , celerity of interface, c_1 [$=\sqrt{gh_1(1+\alpha\beta)}$] corresponds to the stability criteria. It is now difficult to get a single or fixed stability condition including the combined effects of c_1 and c_2. At this stage, it is suggested to consider the maximum value of c_1 and c_2, so that the stability condition proposed here is $\Delta t \le \Delta x / \max(c_1, c_2)$, which shows good agreement with the numerical results as shown in Fig.5.

5. VERIFICATION OF NUMERICAL MODEL

In this section, through comparing the numerical results with the analytical solution, we discuss the validity of this model as well as appropriate boundary condition. In the numerical model, we assume any value of the variables (α, β). However, in our computation the certain condition is selected that α is taken as 0.01, because the analytical solution was found for a certain condition, $\alpha \approx 0$, and the value of β is taken as 1 (i.e. $h_2 = h_1$). The wave amplitude of interface, a , is taken as 1 m, which is small compared with the depth of layer, 25 m. The wave period for both layers is taken as 25.22 sec. Since the periodic condition is used in the analytical solution, the wave period might be assumed in such a way that computational domain become equals to the wave length. For spatial grid points, Δx=10 m, and for temporal grid points, Δt=0.2 sec, have been used.

Initial and Boundary Conditions

As the initial condition, i.e. at t=0, all η_1 and M_1 values are taken as zero. For the interface as shown in Fig.2, the initial condition is set to be the known expression of η_2, which gives

$$\eta_2 = a_2 \sin(kx) \qquad (19)$$

Where, a_2 the amplitude of an interface, and k the wave number.
The corresponding discharge, M_2, for a progressive wave component, was calculated by using the following linear relationship between the water level and discharge :

$$M_2 = D_2 \sqrt{\frac{g}{h_2}} \eta_2 \qquad (20)$$

The numerical solution also depends on the boundary conditions at u/s (upstream) and d/s (downstream) end as well as an initial condition. As mentioned in the stability condition, it is difficult to select the representative celerity in this case. That is why we have a problem to use the characteristic method which requires a specific celerity for setting boundary conditions. In the

present study, four boundary conditions (B.C.) are assumed for the numerical model, based upon the characteristic method with analytical solution and periodic condition. Either discharge or water level for the staggered leap-frog scheme is to be given at the u/s and d/s boundaries. Here we use a discharge.

a) B.C.-1 : Characteristic method-I

The characteristic method is used to estimate M_1 and M_2 at both the u/s and d/s boundaries in each layer. Here the wave celerity representing a slope of characteristics is estimated by values at previous time step again applying the characteristic method.

b) B.C.-2 : Characteristic method-II

The characteristic method is also used at both boundaries in each layer. The wave celerity estimated analytically which is the largest value among two is used throughout the computational domain.

c) B.C.-3 : Combined characteristic method-I and periodic condition

For an upper layer, analytical solution indicates that there are two progressive wave components with different wave celerity. Therefore, at the right boundary, M in each layer is calculated by the characteristic method save as the boundary condition-I. At u/s boundary the same value of water level is given as the same value as the right boundary, which is reasonable for assumed periodic condition.

d) B.C.-4 : Characteristic method-II and periodic condition

The values of discharge at the right boundary, d/s, in each layer are given by B.C.-2. While, at the left boundary the same value of water level is used as right boundary.

Comparison with Analytical Solution

Comparisons between analytical and numerical solutions with different boundary conditions are shown in Fig.6-9. In the numerical model there are two dependent variables, water level and discharge, for each layer. Comparisons are shown only for water level for both top surface and interface.

In general, the agreement between numerical and analytical solutions is fairly good. For an interface the agreement is always very good except for the case of B.C.-2 as shown in Fig.7, where the water level at the left boundary is constant and discrepancy at the right boundary is found. For a top surface agreement is very good for boundary B.C.-1 and 3. But for B.C.-2 and 4 overall agreement is fair. There is a remarkable difference between numerical and analytical solutions at the left and right boundaries. The above result suggests that the characteristic method using the fixed celerity estimated analytically is not applicable because the celerity at boundaries would be varied in time. We should use the characteristic method instead of analytical one to estimate the celerity which is, however, approximate value at the previous time step.

6. NUMERICAL MODEL RESULTS

Effect of Relative Layer Depths

First, simulations with different values of β ($=h_2/h_1$) keeping other parameters (Δx, Δt, α) constant are carried out. Here Δx=10 m, Δt=0.2 sec, and α=0.2 have been assumed. The result are shown in Fig. 10. The interface profile remains same for all values of β, but amplification of a top surface increases with increase in β. Variation of ratio of an amplitude of the top surface to the interface with β is shown graphically in Fig.11.

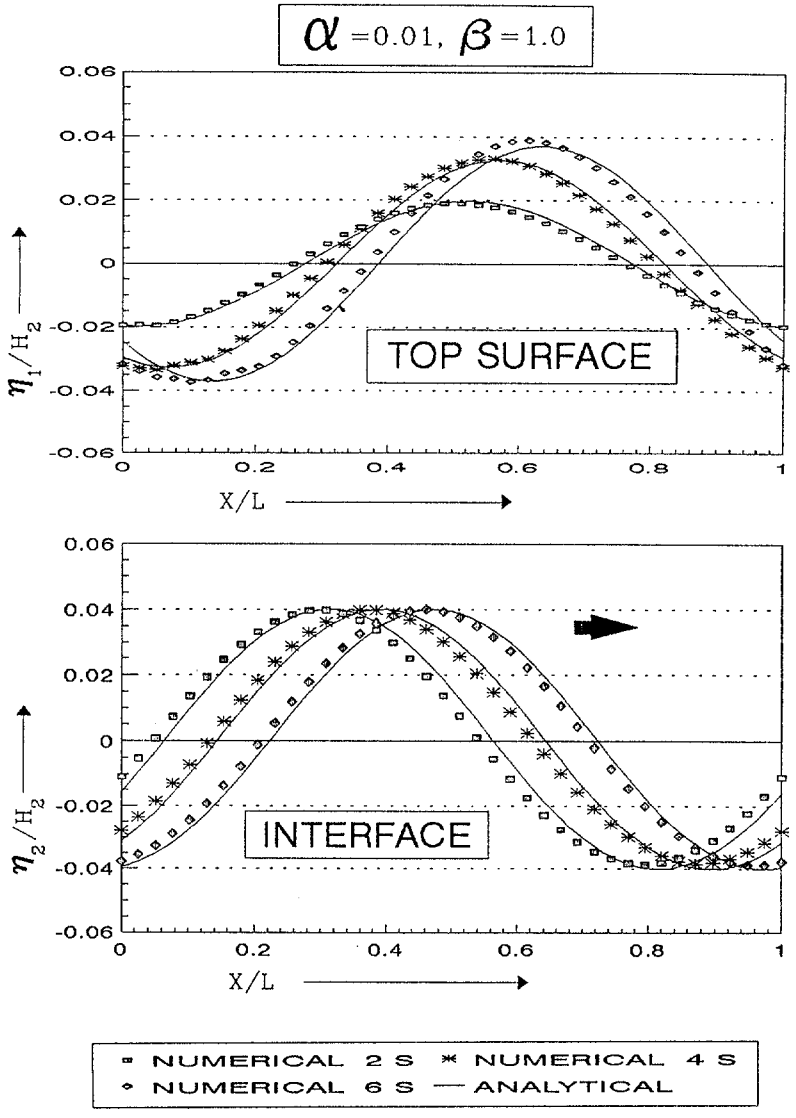

Figure 6 Comparison of analytical and numerical solutions using B.C.-1 with α=0.01 and β=1.0 at t=2,4, and,6 seconds.

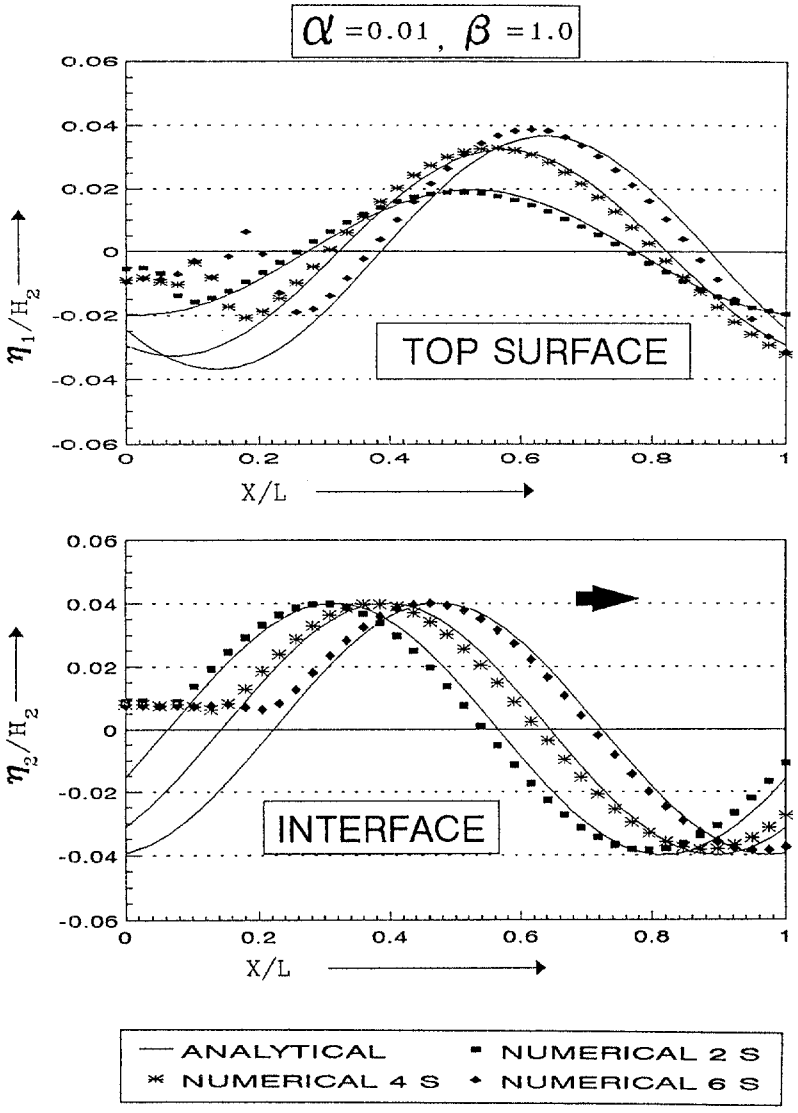

Figure 7 Comparison of analytical and numerical solutions using B.C.-2 with α=0.01 and β=1.0 at t=2,4, and,6 seconds. The discrepancies at the u/s boundary in each layer are significant.

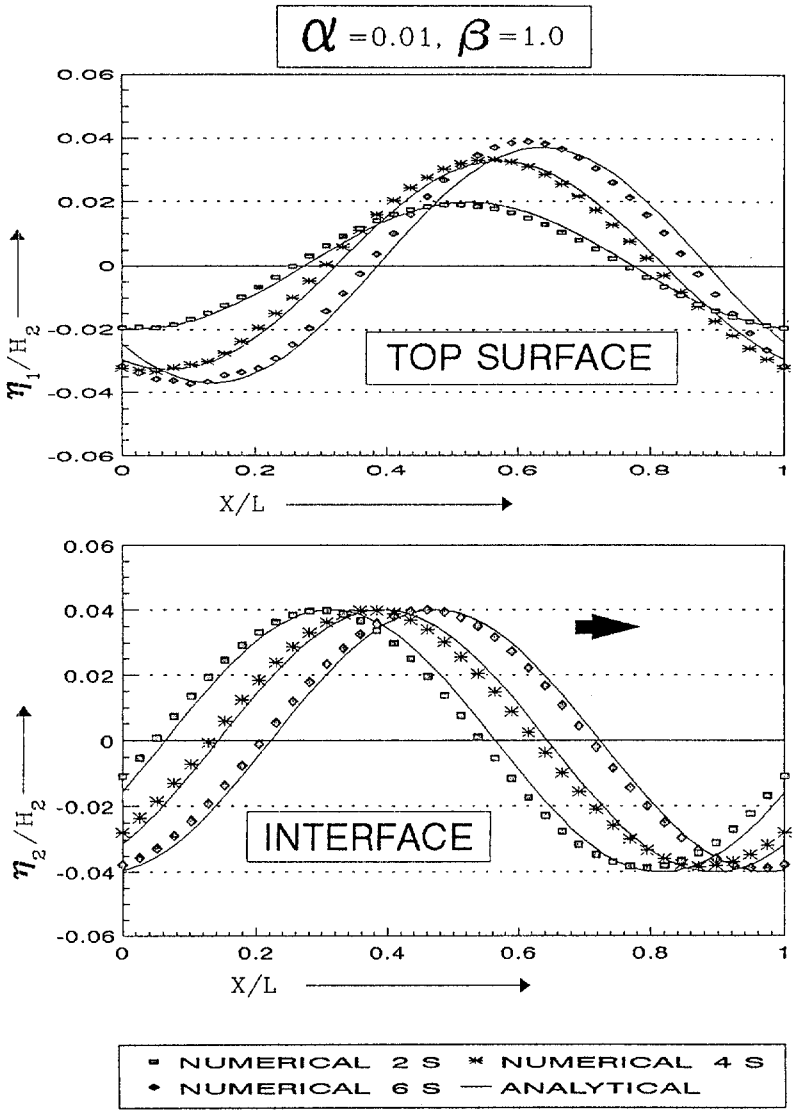

Figure 8 Comparison of analytical and numerical solutions using B.C.-3 with α=0.01 and β=1.0 at t=2,4, and,6 seconds. Numerical oscillation at both boundaries in a top surface is found.

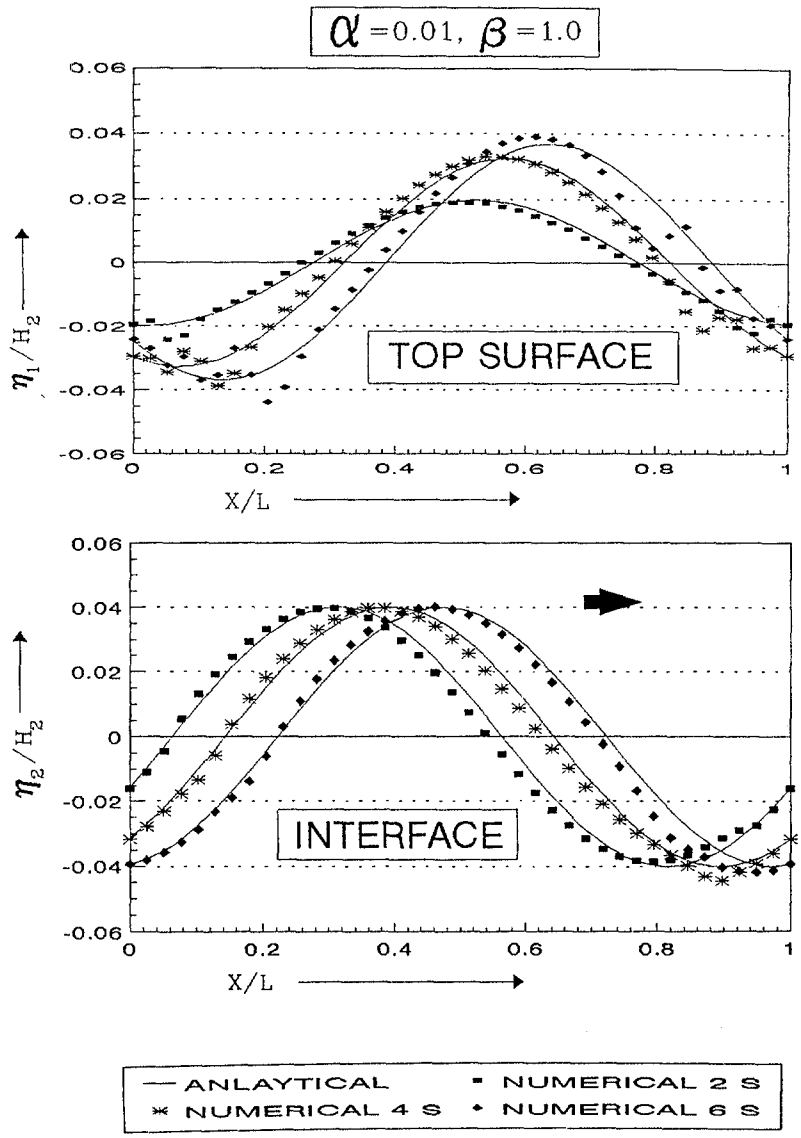

Figure 9 Comparison of analytical and numerical solutions using B.C.-4 with α=0.01 and β=1.0 at t=2,4, and,6 seconds.

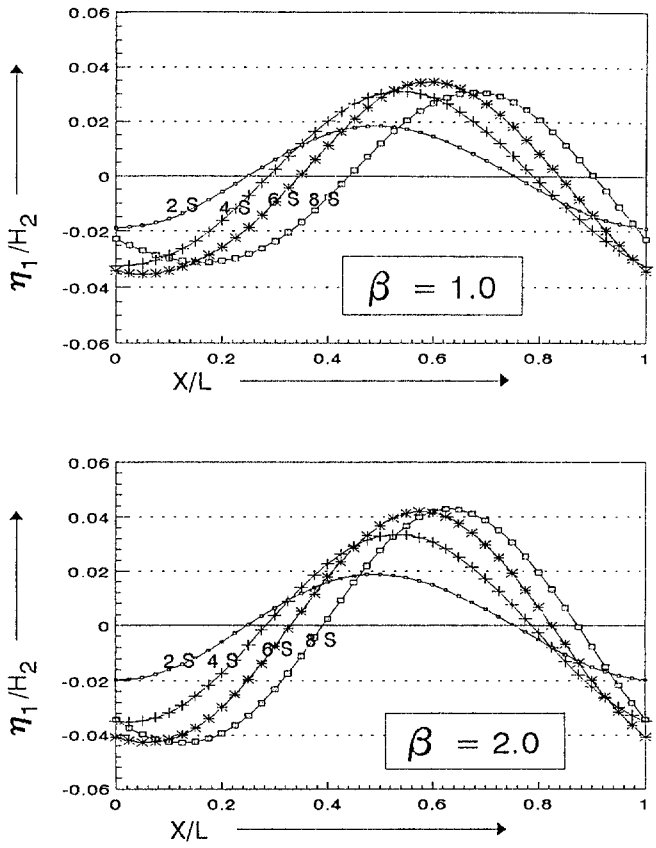

Figure 10 Effect of β on a top surface profile (α=0.2).

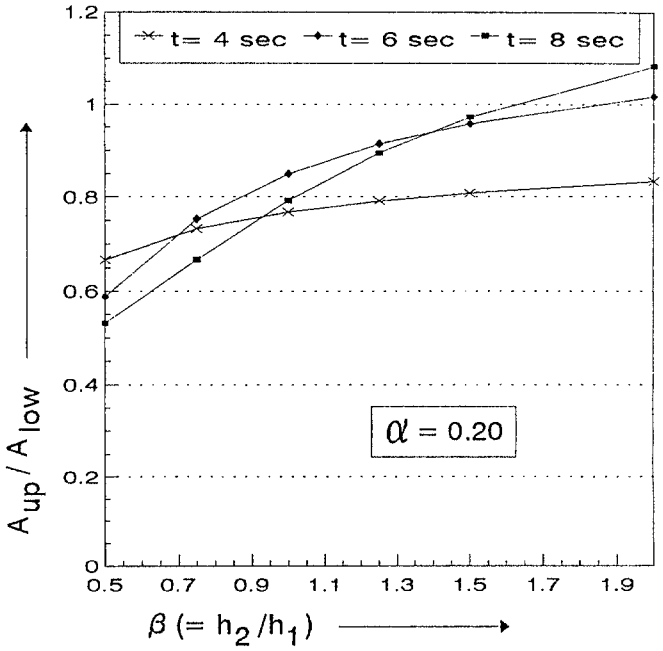

Figure 11 Variation of ratio of amplitudes of top surface to interface with β (α=0.2).

Let us try to explain the above property by the effect of relative layer depth. The last term in left side of Eq.(9) is considered to be the effect by a lower layer on an upper one. Comparing the last term to the second one, gravitational force, in Eq.(9) yields the following ratio :

$$\frac{\beta(1-\alpha)}{(1+\alpha\beta)} \qquad (21)$$

The upper of Fig.12 shows the above function with α and β. As long as the value of α is small, Eq.(21) is approximately equal to β. This means that the external force by a lower layer on an upper layer, the last term in Eq.(9), is proportional to β ,and suggests amplification of the top surface with increase in β. However, it should be remembered that since Eq.(21) doesn't directly show the amplification of the surface, we can only make an overall discussion of the amplification.

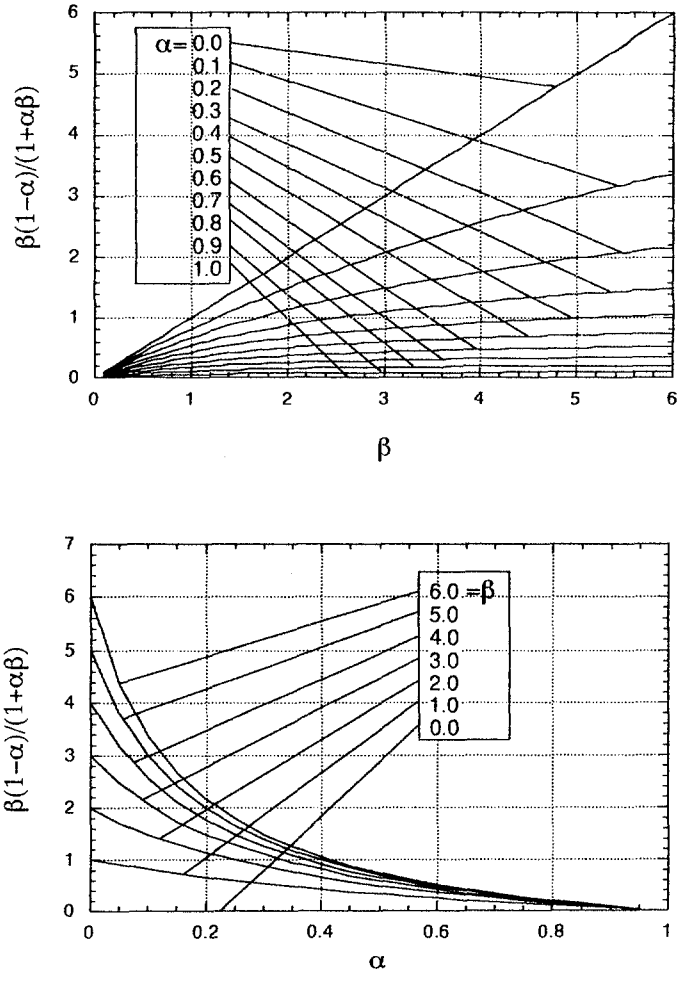

Figure 12 Value of Eq.(21) with α and β, which is the ratio of an external force caused by a lower layer to a gravitational one in an upper one.

Effect of Relative Density

Secondary, simulations with different values of α keeping other parameter (Δx, Δt, β) as constant were carried out. Here Δx=10 m, Δt=0.2 sec, and β=1 were assumed. Figure 13 shows the examples of the wave profile computed with different value of α. It indicates that as α decreases the amplification of top surface also decreases and vice versa. Variation of ratio of amplification of top surface to interface with α is shown graphically in Fig.14. This property can be also interpreted by Eq.(21), showing a top surface linearly decreases with increasing value α for any value of β as shown in the bottom of Fig.12.

The above discussion focuses upon the amplification of a top surface because the major interest in tsunami problems is on the top surface. It is also possible to discuss the other amplification of an interface by using Eq.(10), in which we derive the following ratio by comparing the last term to the second one in Eq.(10) in the same way in Eq.(21) :

$$\frac{\alpha\beta}{(1+\alpha\beta)} \qquad (22)$$

Here we assume the progressive wave component in order to replace the second derivatives with time into that with space. Eq.(22) indicates that an interface could amplify increasing α, which is different from the property of a top surface.

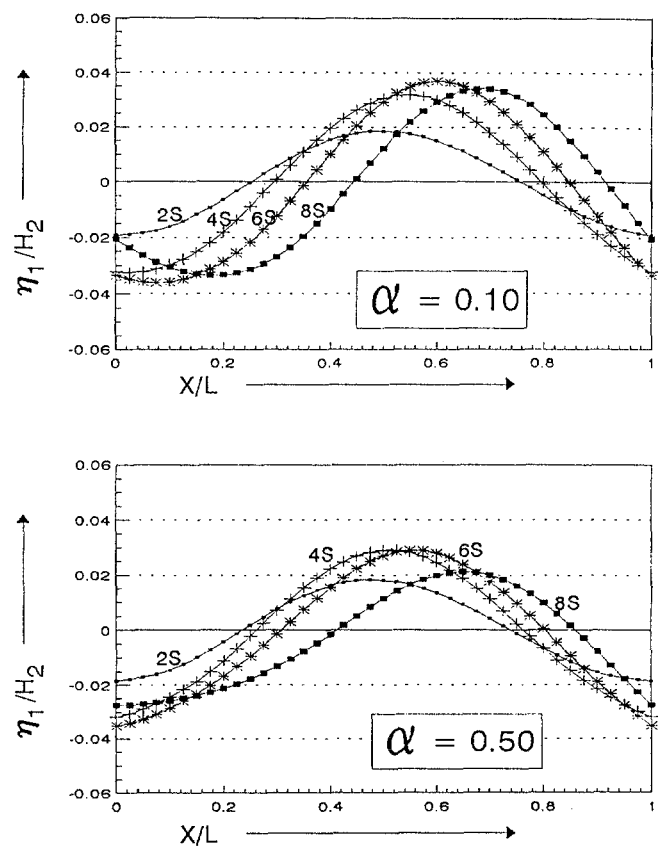

Figure 13 Effect of α on a top surface profile (β=1.0).

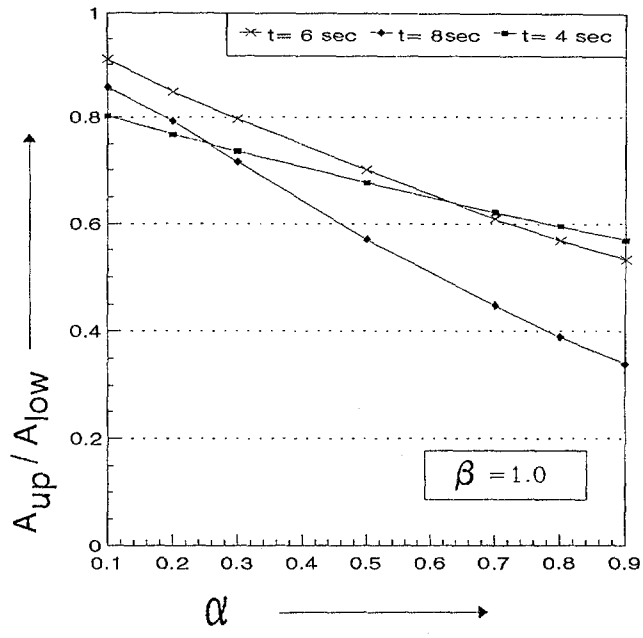

Figure 14 Variation of ratio of amplitudes of top surface to interface with α (β =1.0).

7. CONCLUSION

The governing equations for two-layers were obtained only assuming the long wave approximation. Analytical solution of the linearized equation was derived by using the Fourier transform for a certain condition, negligible ρ_1/ρ_2. This solution contains two progressive waves with different celerities and one reflective wave.

A numerical model is developed using the staggered leap-frog finite difference scheme. Stability condition of the numerical model is discussed and the condition, $\Delta t \leq \Delta x/\max(c_1, c_2)$, is suggested. Accuracy of the linear numerical model is also discussed by comparing the results with an analytical solution. Numerical results depend on the u/s and d/s boundary conditions. If the boundary condition is properly selected, for example, using B.C.-1 and 3, the computed results show a good agreement with the analytical solution. Characteristics of the two-layers model was studied by using it for different conditions with different α and β. It was shown that for lower 'α' and for higher β, an amplification of a top surface increases and vice versa. Both of these phenomena are reasonable and can be explained by physical fluid properties, motive force, Eq.(21).

ACKNOWLEDGEMENT:

This study was partially supported by co-operative research grant from the Ministry of Education, Science and Culture, Japan, and the publication is financially supported by the Ogawa Commemoration Fund.

REFERENCES

AKIYAMA, J., WANG, W. & URA, M. (1990), Numerical Model of Unsteady Gravity Currents, Proc. 7th Congress, APD, IAHR, Beijin.

ELLISON, R.E. AND J.S.TURNER (1959), Turbulent Entrainment in Stratified Flow, J.Fluid Mech., Vol.6, pp.423-448.

HAMPTON, M.H.(1972), The Role of Subaqueous Debris Flow in Generating Turbidity Currents, J. Sedimentary Petrology, Vol.42, No.4, pp.775-793.

HARBITZ,C. (1991), Numerical Simulation of Slide Generated Water Waves, Sci. of Tsunami Hazards, Vol.9, No.1, pp.15-23.

IMAMURA,F.(1995), Review of Tsunami Simulation with a Finite Difference Method, Int.Long Wave Runup Workshop, Friday harbor, Washington, US, 30p..

IMTEAZ, M.M.A. (1993), Numerical Model for the Long Waves in the Two Layers, Master thesis, Asian Inst. Tech., Bangkok, 86p..

JIANG, L. AND P.H.LEBLOND(1992), The Coupling of a Submarine Slide and the Surface Waves Which it Generates, J.Geophys.Res., Vol.97, No.C8, pp.12713-12744.

KRANENBURG, C. (1993), Unsteady Gravity Currents Advancing along a Horizontal Surface, J. Hydraulic Research, Vol.31, pp.49-60.

PARKER ,G.(1982), Conditions for Ignition of Catastrophically Erosive Turbidity Currents, Marine Geology, Vol.46, pp.307-327.

PRANDTL,L.(1952), Essentials of Fluid Dynamics, New York, Hafner.

SIMPSON,J.E.(1982), Gravity Currents in the Laboratory, Atmosphere, and Ocean, Ann.Rev. Fluid Mech., Vol.14, pp.213-234.

TURNER, J.S. (1973), Buoyancy Effects in Fluids, Cambridge University Press, Cambridge, 367p..

Let us derive the governing equations for long waves in two-layers using the Euler equation neglecting viscous effect, which is composed of two kinds of equations; the mass and momentum continuity equations. In the case of x-z plane as shown in Fig.1, they are given by the following equations in each layer:

$$\frac{\partial u_i}{\partial x}+\frac{\partial w_i}{\partial z}=0 \qquad \text{(A1)}$$

$$\frac{\partial u_i}{\partial t}+u_i\frac{\partial u_i}{\partial x}+w_i\frac{\partial u_i}{\partial z}=-\frac{1}{\rho_i}\frac{\partial p_i}{\partial x} \quad \text{(x-component)} \qquad \text{(A2)}$$

$$\frac{\partial w_i}{\partial t}+u_i\frac{\partial w_i}{\partial x}+w_i\frac{\partial w_i}{\partial z}=-g-\frac{1}{\rho_i}\frac{\partial p_i}{\partial z} \quad \text{(z-component)} \qquad \text{(A3)}$$

where p is the fluid pressure, ρ the density of fluid, i =1 (upper layer) or 2 (lower layer). Considering a function along streamline which is constant with time, and differentiating it with respect to time, the kinetic boundary conditions at a top surface, an interface, and a bottom are given as follows :

$$\text{at } z=\eta_1 , \quad \frac{\partial \eta_1}{\partial t}+u_1\frac{\partial \eta_1}{\partial x}=w_1 \quad \text{(A4)}$$

$$\text{at } z=\eta_1-h_1 , \quad \frac{\partial \eta_2}{\partial t}+u_1\frac{\partial \eta_2}{\partial x}=w_1+u_1\frac{\partial h_1}{\partial x} \text{ and } \frac{\partial \eta_2}{\partial t}+u_2\frac{\partial \eta_2}{\partial x}=w_2+u_2\frac{\partial h_2}{\partial x} \qquad \text{(A5)}$$

$$\text{at } z=-(h_1+h_2), \quad u_2\left(\frac{\partial h_1}{\partial x}+\frac{\partial h_2}{\partial x}\right)=-w_2 \qquad \text{(A6)}$$

The dynamic condition of the continuity of pressure are added for the boundary condition at a top surface and an interface. Since the air pressure is assumed to be zero, those conditions are expressed by

$$\text{at } z=\eta_1 , \quad p_1=0 \quad \text{(A7)}$$

$$\text{at } z=\eta_1-h_1 , \quad p_2=\rho_1 g(\eta_1+h_1-\eta_2) \quad \text{(A8)}$$

Integration of Eqs.(A1) and (A2) yields Eqs.(1)-(4). For example, the mass continuity equation in an upper layer is derived from Eq.(A1)using by the Leibniz rule and boundary conditions in Eqs. (A4) and (A5) :

$$\int_{\eta_2-h_1}^{\eta_1}\left(\frac{\partial u_1}{\partial x}+\frac{\partial w_1}{\partial z}\right)dz$$

$$=\frac{\partial}{\partial x}\int_{\eta_2-h_1}^{\eta_1}u_1dz-u_1\frac{\partial \eta_1}{\partial x}\bigg|_{z=\eta_1}+u_1\frac{\partial(\eta_2-h_1)}{\partial x}\bigg|_{z=\eta_2-h_1}+w_1\big|_{z=\eta_1}-w_1\big|_{z=\eta_2-h_1}$$

$$=\frac{\partial M_1}{\partial x}-u_1\frac{\partial \eta_1}{\partial x}\bigg|_{z=\eta_1}+u_1\frac{\partial \eta_2}{\partial x}\bigg|_{z=\eta_2-h_1}-u_1\frac{\partial h_1}{\partial x}\bigg|_{z=\eta_2-h_1}+w_1\big|_{z=\eta_1}-w_1\big|_{z=\eta_2-h_1} \quad \text{(A9)}$$

$$=\frac{\partial M_1}{\partial x}+\frac{\partial \eta_1}{\partial t}+u_1\frac{\partial h_1}{\partial x}\bigg|_{z=\eta_2-h_1}-\frac{\partial \eta_2}{\partial t}-u_1\frac{\partial h_1}{\partial x}\bigg|_{z=\eta_2-h_1}$$

$$=\frac{\partial M_1}{\partial x}+\frac{\partial(\eta_1-\eta_2)}{\partial t}=0$$

UNDERWATER LANDSLIDES INEFFECTIVE AT TSUNAMI GENERATION.

Paul H. LeBlond,
Department of Oceanography
University of British Columbia, Vancouver, B.C., Canada

Anthony T. Jones,
Oceanus Flotation Technologies
Suite 1401, 1166 Alberni St., Vancouver, B.C., Canada

ABSTRACT

Underwater landslides of deformable sediments have been shown to be relatively ineffective at generating sea surface waves. Calculations of tsunamis waves which assume that the sliding mass behaves like a rigid body are bound to be overestimates. We apply this principle to the discussion of the hypothetical 105 Ka Lanai tsunami.

The assumption that a giant wave, presumably a locally generated tsunami, was responsible for the presence of marine deposits 326 meters above present sea-level on Lanai certainly does not meet universal approval (1,2). Other hypotheses have been put forward to explain the location of this material: uplift of the islands, or transport of the material by native Hawaiians (3,4).

Testing the situation through physical modeling is clearly a step forward in assessing whether such a large wave could have been generated by observed subsurface displacements. The model presented in (5) shows that the estimated volumes of local submarine landslides are not quite sufficient to the task. We wish to point out another point relevant to tsunami generation by submarine landslides.

Submarine landslides usually result from slumping of unconsolidated sediments which fall along the sloping sea floor until they accumulate downhill in a flat area. The adjustment of the sea floor takes a time which is not negligible on the time-scale of sea surface displacements, and thus

cannot be adequately modelled as an instantaneous volume-preserving re-arrangement of the bottom boundary. Jiang and LeBlond (6,7,8) have examined the coupled problem of underwater avalanches and the surface waves which they create. They found that the rheology of the sliding material is an important factor in determining the effectiveness of the landslide in generating a tsunami. Less viscous material slides faster and causes larger waves. In general, the waves produced by sliding deformable material are smaller than those produced by undeformable materials (for example, as in the experiments of Wiegel (9) and the calculations of Tuck and Wang (10). Although no direct comparison has been made between the wave generation potential of an underwater slide and that of an instantaneous displacement of the bottom to a configuration resulting from the effect of that slide, one would expect the former, slower phenomenon to be much less effective at making waves than the latter.

The calculations presented in (5), which take for initial conditions an instantaneous sea-floor re-arrangement, must thus be high upper bounds on the size of the surface waves generated by the Alika 2 slide. That even those waves do not suffice to reach the required level speaks strongly against a landslide-generated tsunami explanation for the Lanai marine deposits.

REFERENCES

1. George W. Moore and James G. Moore, "Large scale bedfroms in boulder gravel produced by giant waves in Hawaii, Geological Society of America Special Paper 229, pages 101-110 (1988).

2. James G. Moore, David. A. Clague, Robin T. Holcomb, Peter W. Lipman, William R. Normark and Mark E. Torresan, "Prodigious submarine landslides on the Hawaiian Ridge", Journal of Geophysical Research, Vol 94, pages 17,465 - 17, 484 (1989).

3. Anthony T. Jones,"Elevated fossil coral deposits in the Hawaiian Islands: A measure of island uplift in the Quaternary". Ph.D. Dissertation, University of Hawaii, 274 pp. (1993).

4. Anthony T. Jones and Richard W. Grigg, "Lithospheric flexure in Hawaiian archipelago as revealed by elevated coral terraces". (in press) (1995).

5. Carl Johnson and Charles L. Mader, "Modeling the 105 Ka Lanai Tsunami", Science of Tsunami Hazards, Vol 12, pages 33-36 (1994).

6. Lin Jiang and Paul H. LeBlond, "The coupling of a submarine slide and the surface waves which it generates", Journal of Geophysical Research, Vol 97, pages 12,731- 12,744 (1992).

7. Lin Jiang and Paul H. LeBlond, "Numerical modeling of an underwater Bingham plastic mudslide and the waves which it generates", Journal of Geophysical Research, Vol 98, pages 10,303-10,317 (1993).

8. Lin Jiang and Paul H. LeBlond, "Three-dimensional modeling of tsunami generation due to a submarine landslide", Journal of Physical Oceanography, Vol 24, pages 559-572 (1994).

9. R.L. Wiegel, "Laboratory studies of gravity waves generated by the movement of a submerged body" EOS Transactions American Geophysical Union, Vol 36, pages 759-774 (1955).

10. E.O. Tuck and L.S. Hwang, "Long wave generation on a sloping beach", Journal of Fluid Mechanics, Vol 51, pages 449-461 (1972).

MATHEMATICAL MODELING IN MITIGATING THE HAZARDOUS EFFECT OF TSUNAMI WAVES IN THE OCEAN. A PRIORI ANALYSIS AND TIMELY ON-LINE FORECAST(*)

Yurii I. Shokin, Leonid B. Chubarov

Institute of Computational Technologies,
Siberian Division of the Russian Academy of Sciences
6, Lavrentyev Ave., Novosibirsk, 630090, RUSSIA

ABSTRACT

The paper deals with the mathematical models applied to the studies of wave regimes in a wide range of parameters of water areas and initial perturbations, and the calculation of dynamic and kinematic wave characteristics.

Special attention is paid to the solution of specific problems including the development of the application software for computer-aided tsunami warning system on the Pacific coast of Russia. Program structures and information fields are described and sample test calculations are presented.

Mathematical modeling in such problems was used for zoning Kuril-Kamtchatka coast of Russia with respect to their vulnerability and for parameter calculations for Local Tsunami Warning System in one of the Pacific water areas near Kamtchatka.

The software system for on-line forecast of tsunami travel times has been used in the operation of Sakhalin and Kamtchatka Tsunami Warning Centers and its basic algorithms have been employed during the preparation of the Atlas of tsunami travel charts for the Pacific Tsunami Warning System developed by the order of IOC UNESCO.

All the algorithms have been tested on model tasks and their accuracy has been estimated. In particular, the error of the determined tsunami travel time does not exceed 3-4 minutes per hour of wave propagation.

(*) The investigation has been supported by the Foundation of Fundamental Research of the Russian Federation (94-05-1628a)

1. INTRODUCTION

Computational experiment in tsunami problems is specified by the multifactor physical process including the generation of the initial perturbation (tsunami source) resulting from an underwater earthquake, volcano eruption or another similar large-scale hazard, propagation of the wave in deep ocean and its transformation in the coastal zone, interaction with floating and fixed objects and its running up the shore.

The applied tsunami problems differ in content. One of them is associated with carrying out a priori investigations, such as the coast zoning according to vulnerability, parameters calculation for local, regional and global tsunami warning systems, preparation of charts of inverse isochrones, scenario calculations.

Another group of problems is determined by the needs of on-line forecast and monitoring of tsunami and involves the development of mathematical models, algorithms and applied software for the reception and processing of continuously incoming information as well as for the expert assessment of the current situation in the ocean, development of the tsunami service regulations and designing the text forms of specially issued messages.

2. A PRIORI ANALYSIS

2.1. BASIC MATHEMATICAL MODELS

Transformation modeling of long surface gravitational waves is mostly carried out within the scope of the shallow water theory. Depending on the intervals of characteristic parameter change different approximations of this theory are to be considered such as linear, nonlinear and nonlinear-dispersive.

Very important is the construction of a hybrid mathematical model which can describe the wave transformation during its propagation from the perturbation source to the coast with automatic adjustment to a specific algorithm according to the current wave characteristics and the zone of the water area where it is propagating.

Such a model must include approximated hydrodynamic shallow water models and complete hydrodynamic equations fully allowing for vertical displacements of fluid.

The construction of an efficient hybrid model requires the development of the selection criteria of its individual components, algorithms of joining the solutions and boundary conditions describing the entire variety of simulated physical phenomena (open boundaries, interaction with floating and fixed objects, running of the waves up the shore). At the same time we must proceed from the reliability requirements to the wave processes reproduction as well as from time and effort sparing computational algorithms which must make it possible to carry out a priori and on-line modeling.

Dispersion effects and their interaction with nonlinearity effects can be correctly allowed for by means of the models whose dispersive properties are retained within a

wide range of the wavelength changes and the notation and type of the output assertions enable one to employ efficient stable algorithms in a two-dimensional (planned) statement.

In parametric form the equations of the shallow water theory, in particular, nonlinear-dispersive Aleshkov model can be written as follows:

$$\begin{aligned}
&\eta_t + \nabla\cdot\left[(h+r\eta)\vec{u}\right] = \\
&\quad = s\Big\{(\vec{u}\cdot\nabla h)\left|\nabla h^2\right| + h\Big[\left|\nabla h^2\right|(\nabla\cdot\vec{u}) + 2\nabla h\cdot\nabla(\vec{u}\cdot\nabla h) + (\vec{u}\cdot\nabla h)\Delta h\Big] + \\
&\quad +0.5h^2\left[\Delta(\vec{u}\cdot\nabla h) + 2\nabla h\cdot\nabla(\nabla\cdot\vec{u})\right] + \left(h^3/6\right)\left(\Delta(\nabla\cdot\vec{u})\right)\Big\}, \qquad (1)\\
&\vec{u}_t + \nabla\left(g\eta + 0.5r\left(\vec{u}^2\right)\right) = 0.5s\nabla\left[(\vec{u}\cdot\nabla h)^2 + \nabla\cdot\left(h^2\vec{u}_t\right)\right],
\end{aligned}$$

where η is the deviation of the free surface from its undisturbed level, h stands for the depth of undisturbed water level, $\vec{u}$ designates the vertically averaged velocity component, Δ, ∇ are two-dimensional in the plane (x, y) Laplace and gradient operators, respectively, g is the acceleration of gravity, r and s denote parameters such that:

$r = 0$, $s = 0$ for a linear model;

$r = 0$, $s = 1$ for a linear-dispersive model;

$r = 1$, $s = 0$ for a nonlinear model;

$r = 1$, $s = 1$ for a nonlinear-dispersive (NLD) model.

Let us dwell upon some unusual nonlinear-dispersive models of shallow water expanding the class of solvable problems. Thus A.Urusov and Yu. Shokin [1] suggested a model within which the interaction of waves with a fixed partially submerged body can be described. Equations of the model are the consequences of Eqs. (1) under the assumption of the smallness of the wave amplitude:

$$\begin{aligned}
&\eta_t + \nabla\cdot\left(H\nabla\varphi\right) = 0.5\mu\nabla\cdot\Big\{\nabla\left(h^2\nabla\varphi\cdot\nabla h\right) + h^2\nabla h\Delta\varphi + \\
&\quad +\left(h/(3g)\right)\nabla\left[\left(\varphi_{tt} - \nabla h\cdot\nabla\varphi\right)/h\right]\Big\} + O\left(\varepsilon\mu, \mu^2\right), \\
&\left(\varphi - 0.5\nabla\cdot\left(h^2\nabla\varphi\right)\right)_t + g\eta + 0.5\varepsilon\left|\nabla\varphi\right|^2 + O\left(\varepsilon\mu, \mu^2\right) = 0, \qquad (x,y)\notin\omega, \qquad (2)\\
&\nabla\cdot\left(d\nabla\psi\right) = \mu\nabla\cdot\Big\{d\nabla d\left(\nabla\psi\cdot\nabla d\right) + 0.5d^2\left[\left(\nabla d\Delta\psi\right) + \nabla\left(\nabla\psi\cdot\nabla d\right)\right] + \\
&\quad +\left(d^3/6\right)\nabla\left(\Delta\psi\right)\Big\} + O\left(\mu^2\right), \qquad (x,y)\in\omega.
\end{aligned}$$

We also take that φ designates the potential value at the bottom of the pool outside the partially submerged body, ψ denotes the same but in the area ω i.e. under the body, $H = h+\eta$ is the total depth, $d = d(x, y)$ is the height of the gap between the

bottom and the body, A_0 and H_0 denote the characteristic wave amplitude and the depth of the water area, L_0 is the characteristic horizontal dimension, μ and ε are parameters such that

$$\mu = (H_0 / L_0)^2, \ \varepsilon = A_0 / H_0 .$$

The conjugation conditions on the areas interface result from the requirement of potential and pressure continuity.

The suggested equations ensure the approximation with an accuracy of $O(\varepsilon\mu, \mu^2)$. In model derivation we assumed also that $\varepsilon / \mu = O(1)$.

The formulation of the Eqs. (1) in terms of the wave height (η) and potential (φ, ψ) lowers the order of space derivatives entering into these equations and makes it easier to construct computational algorithms.

A one-dimensional analogue of model (2) was successfully employed in the solution of some test and simulation problems [2].

At the same time it is vitally important to work out algorithms for the on-line calculation of the dynamic characteristics such as tsunami heights and velocities. Such algorithms must be very efficient, i.e. they must be able to simulate the wave propagation over transoceanic distances in the on-line operation mode ahead of the real wave propagation and allow for the nonlinearity and dispersion effects which become the crucial factor under the description of the global-scale wave processes.

This accounts for the wide use of NLD models which, unfortunately, are realized by means of awkward and cumbersome computational algorithms which hinders the on-line operation. One of the possible ways out would be in making use of an approximated NLD model suggested in [3].

$$\eta_{tt} - g\nabla \cdot (h\nabla\eta) = -f^2\eta + \nabla \cdot \left(h\nabla(h\eta_{tt})\right) / 3 + 3g\nabla \cdot \left(h\nabla\left(\eta^2 / h\right)\right) / 2 , \qquad (3)$$

where f is Coriolis parameter.

In this work so-called absorbing boundary conditions are suggested that to be enable for simulating the wave propagation along the route from the source to the coast by means of the "running" window. Application of model (3) is reduced to the solution of a single equation for η which, nevertheless, provides means for taking into account various dispersion factors such as the effect of the rotation of the Earth, nonlinear and frequency dispersion.

Note also the possibilities of the NLD model construction which takes into account the influence of the water area bottom porosity on the wave process.

A one-dimensional analogue of such a model suggested in [4] has the following form:

$$u_t + \left(u^2/2\right)_x + g\eta_x = \left[\left(0.5h^2u\right)_{xx}\right]_t ,$$
$$\eta_t + \left[(h+\eta)u\right]_x = \left[h_x u_t - (H_0 - h)u_{xt}\right] / \rho + \left(h^3 u / 6\right)_{xxx} , \quad (4)$$

where $\rho = \nu / \aleph$, ν is the kinematic viscosity and $\aleph$ denotes the permeability of the porous medium.

2.2. METHODOLOGICAL PRINCIPLES OF SOME COMPUTATIONAL EXPERIMENTS IN TSUNAMI PROBLEMS.

2.2.1. A PRIORI ZONING OF THE COAST

A priori zoning of the coast with respect to the vulnerability to hazardous waves is known to require determination of location, intensity and main peculiarities of the mechanism of perturbation sources and analyzing the quantitative characteristics of the waves at individual coastal points. The natural input data in this case will be historical data and the measurements of the level whose interpretation may result in the long-term local forecast for the points of reference, i.e. for the given period of a forecast t_* and the value of the level h_{t_*}:

$$h_{t_*}(x_i) = F_1\left(x_i; t_*, k(x_i), A, T\right),$$

where coefficients A and T are "regional" parameters that determine the wave behavior in shallow water: A denotes the recurrence of major events in the studied region, T stands for the predominant wave period, coefficient $k(x_i)$ is associated to the route of the wave propagation and characterizes the local singularities of the protected point (x_i) location.

Then the problem is reduced to the calculation of the function

$$H_{t_*}\left(x_i, x_j\right) = H\left(F_1, K\left(x_j\right)\right)$$

along the investigated coast at the points (x_j) with respect to "reference" values $h_{t_*}(x_i)$ where $K(x_j)$ is the recount coefficient from point to point along the coast. The computational experiment in this case consists in the assessment of the above mentioned fundamental parameters and obtaining the function F_1, i.e. building up the model of a priori forecast.

The series of computational experiments based on the above considered mathematical models involves scenario calculations of the waves propagation from the hypothetical (critical) sources and simulation of real events. The finite result in this case is scarcely affected by the input conditions because in the prognostic model the so-called "effective" wave source is considered whose parameters in the deep water do not change much from point to point, i.e. are stable characteristics within the assumed prognostic model. The accuracy of the estimated coefficients $k(x_i)$ and $K(x_j)$ is directly related to the employed mathematical models and numerical algorithms.

2.2.2. ON-LINE ASSESSMENT OF THE HAZARDOUS WAVE PARAMETERS

The second group of problems connected with the calculation of the safety criteria of objects depends on the requirements of the real-time monitoring of the hazardous process. The suggested approach involves the organization of a rational location scheme of deep-water hydrophysical gauges for early detection of dangerous waves, the development of methods for reliable and timely analysis of the recorded data, their interpretation in prognostic terms.

Therefore, local on-line forecast consists in the estimation of the level $h_{t*}(x_i)$ at the protected point (x) which is obtained from the observation data of the wave characteristics on the local system gauge:

$$h_{t_\alpha}(x) = F_2\left(x; t_\alpha, k(x), \alpha, \tau\right),$$

where t_α is the parameter which determines the minimum time required for decision-making and taking measures of protection. The parameters α, τ are the wave amplitude and period registered by the gauge; $k(x)$ is the coefficient of the wave transformation from the gauge to the protected point (x).

To avoid uncertainty associated with the perturbation source on solving this problem is possible taking the wave characteristics (α, τ) being stable in the deep water from the gauges' measurements. The coefficient $k(x)$ characterizes the local conditions and specific manifestations of the wave nearby the protected point.

The reliability of the prognostic model F_2 built as described above is determined by the algorithmic support of the numerical experiment and the completeness of the natural data. The model includes nomograms for the estimation of the probable tsunami travel time and the flooded zones at the protected point.

2.3. COMPUTATIONAL EXPERIMENT FACILITIES EMPLOYED FOR THE TRAINING OF THE TSUNAMI WARNING SERVICE PERSONNEL AND OF THE POPULATION IN THE THREATENED ZONES

The qualification requirements to the tsunami warning services and similar services intended for warning the population in the case of natural and man-made hazards as well as to their equipment for monitoring and investigation of hazardous processes are becoming greater and greater. It necessitated the development of software systems intended for scenario calculations illustrating the possible variants of catastrophic events depending on the characteristics of a physical phenomena, specific features of the protected points and the operation of the local administration, professional retraining of the special services personnel.

Training programs (TP) development in the considered fields involving rather complex physical phenomena and accordingly non-trivial mathematical models and computational algorithms are of special interest.

The TP structure involves the mathematical simulation facilities, interface, training, analysis of results and work with data bases.

TPs due to their specific functions require allowing for the psychological peculiarities of the user which makes TP significantly differ from the Applied Packages (AP) with respect to the selection of mathematical models and computational algorithms. This necessitates the selection of simple mathematical models retaining, at the same time, reliability of the reproduction of essential characteristics of a phenomenon, making use of computational algorithms which can operate within a wide range of input data and model parameters.

We must name also such specific features of the TPs as some forced limitation of the input data range due to the requirements of guaranteed stability and accuracy of calculations, adjustment to particular objects of the users' professional activity and the strict discipline of the control in order to train the necessary skills and habits of working with applied programs and obtaining meaningful results.

The authors made use of the above consideration in the development and operation of TP "Tsunami" which ensures successful study of hydrodynamic problems associated with tsunami, peculiar features of the waves behavior in the protected zones within the responsibility of specific services, possibilities of prevention and protection from the hazardous consequences of tsunami.

3. TIMELY ON-LINE FORECAST.

Timely tsunami warning efficiency can be improved and the National Tsunami Warning Service (TWS) can become integrated into the respective international structures only by means of new algorithms, software and hardware.

By way of example of such software and hardware tool-kit, let us consider the EVENT system [5].

The hardware is based primarily on two workstations of the IBM PC/AT 286 or 386 type or fully compatible with them. One of them at the same time is operated by the duty oceanologist (it will further be referred to as "the host") and the other (further referred to as "the slave") is operated by the technical staff of the TWS.

Here we shall consider the software tool-kit for the oceanologist on duty. The second component has been developed by the Central Designing Bureau of Russian Hydrometeorological Center and partially described in Ref. [6]. All the software subsystems are supported by MS DOS version 3.30 or later.

The software tool-kit of the "host" provides the reception and checking of data on tsunamigenic earthquake, and determination of the respective warning procedure, timely calculation of the tsunami travel times, refined direct simulation of the wave propagation allowing for the characteristics of the source of the present earthquake,

transmission of the calculation results to the TWS technical staff's workstation, maintaining the user's interface and the visualization of the results.

3.1 BASIC CALCULATION ALGORITHMS

When choosing an algorithm for the timely calculation of the tsunami travel time the authors proceeded from the natural assumption of the equality of these times under the propagation of the waves from the source to the coastal points and back.

The calculation algorithm adopted by the authors for the calculation of the inverse isochrones tables is based on the well-known Huygens method and is actually a group of methods which obtain the time required for passing the given space interval with the given speed.

Under construction, all the nodes of the calculated grid are partitioned into three sets, Set M_1 contains the nodes with finally calculated tsunami travel times, M_2 – the nodes with preliminary estimated values that may later be refined and M_3 – the nodes with arrival times that has not been obtained yet.

Each node U is associated with the notion of its domain of influence S_U (pattern), i. e. the aggregate of neighboring nodes satisfying some criterion of proximity (see Fig. 1). It is considered that during one step of an algorithm the perturbation can cover the distance from the specified node only to its nearest pattern neighbors.

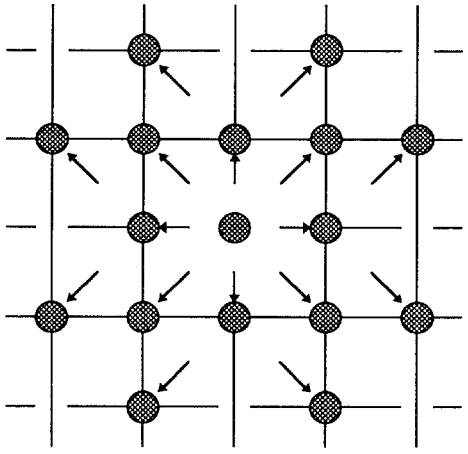

Fig.1. 17-point pattern

At the initial time all the nodes in the domain of the initial perturbation are assigned the zero value of the arrival time (or time T_0, i. e. the time of the beginning of the earthquake) and included in the set M_2^0. The remaining nodes of the calculation domain are included in M_3^0. Then the nodes of the M_2^0 with patterns not influenced by the ones of the set M_3^0 are transferred to the set M_1^1 and excluded from the further calculations. It concludes the preliminary stage of the algorithm that afterwards acquires the regular character.

Thus, at the n-th step the exhaustive search of the nodes from the set M_2^n is performed in order of increasing tsunami travel times known at this moment.

Let the node $A \in M_2^n$ and

$$T_A = \min_{A_i \in M_2^n} \{T_{A_i}\}, \tag{5}$$

then for the node B such that $B \in S_A$ the tentative estimate A of the arrival time is found from the formula

$$T = T_A + T_{AB}, \tag{6}$$

where $T_{AB} = \dfrac{2L_{AB}}{C_A + C_B}$ is the time of the perturbation propagation from the node A to node B,

$$L_{AB} = R * \arccos(\sin\varphi_A * \sin\varphi_B + \cos\varphi_A * \cos\varphi_B * \cos\Delta\psi) \tag{7}$$

denotes the distance from A and B nodes through an arc of the great circle and R stands for the radius of the Earth, $C = \sqrt{gh_i}$ is the local rate of perturbation propagation, h_i designates the depth in the i-th node, g is the acceleration of gravity.

If $B \in M_3^n$, then the relation (5) first yields the value of T and the node B itself is transferred to M_2^{n+1}, if $B \in M_2^n$, the value of T is refined from the minimizing relation

$$T_B = \min_{A \in S_B \cap M_2^n} \{T_A, T_A + T_{AB}\}. \tag{8}$$

After the values of T, $\forall B : B \in S_A$, are obtained from Equations (5) and (6), the node A is transferred to the set M_1^{n+1}. This procedure is repeated for the next node $A \in M_2^n$, satisfying the condition (5) and so on until the set M_2^n is exhausted. At the next $n+1$-th step the algorithm is reproduced without any changes and the calculation goes on until at some step k all the calculation nodes of the water area are included in the set M_1^k.

The resulting tables of the tsunami travel times are used for obtaining the respective time characteristics and the development of the isochrone charts.

For detailed research the method of the calculation of tsunami travel times from the specific source has been developed based on the eikonal equations [7].

$$\frac{d\varphi}{d\tau} = q\frac{H}{H_0}, \quad \frac{d\psi}{d\tau} = \frac{H}{H_0}\frac{p}{\cos^2\varphi}, \quad \frac{dp}{d\tau} = -\frac{1}{2H}\frac{dH}{d\psi}, \quad \frac{dq}{d\tau} = -\frac{1}{2H}\frac{dH}{d\varphi} - \frac{H}{H_0}\frac{\sin\varphi}{\cos^3\varphi}p, \tag{9}$$

which, together with the initial conditions

$$\varphi|_{\tau=0} = \varphi_0, \quad \psi|_{\tau=0} = \psi_0, \quad p|_{\tau=0} = \sqrt{\frac{H_0}{H}}\cos\varphi_0\cos\gamma, \quad q|_{\tau=0} = \sqrt{\frac{H_0}{H}}\sin\gamma, \tag{10}$$

enable one to find the trajectory of ray motion from the perturbation source at some angle γ.

Here (φ, ψ) are the current geographical coordinates (longitude and latitude), H_0 is the average ocean depth, H is the current ocean depth, $\tau = \frac{\sqrt{gH_0}}{R}t$, $p = \frac{R}{\sqrt{gH_0}}p'$, $q = \frac{R}{\sqrt{gH_0}}q'$ denote the dimensionless time and characteristic variables.

The isochrone charts are made in this case as follows: a family of trajectories with different initial deflections is emitted from the perturbation source, and then the system of equations (9) and (10) is solved sequentially. The set of the values of (φ, ψ) calculated at the given moment of time produces the corresponding isochrone.

3.2. BASIC SOFTWARE COMPONENTS

The basic component of the software supporting the workstation of the TWS duty oceanologist is the program START containing program units assuring the functioning of the subordinate program modules and the information exchange between different components of the software tool-kit. The structure of the START program is plotted on the Fig. 2.

The program unit INIT describes the global variables, initializes parameters, assignment and preservation of the environment state, setting of the used interruption vectors, processing of critical situations and ensures the program integrity in case of the hardware malfunctions.

Program unit VIEW_EV contains interpolation procedures for the determination of the tentative tsunami travel times from the tables of the inverse isochrones and the direct modeling of kinematics of the wave propagation from the "real" source of the tsunamigenic earthquake.

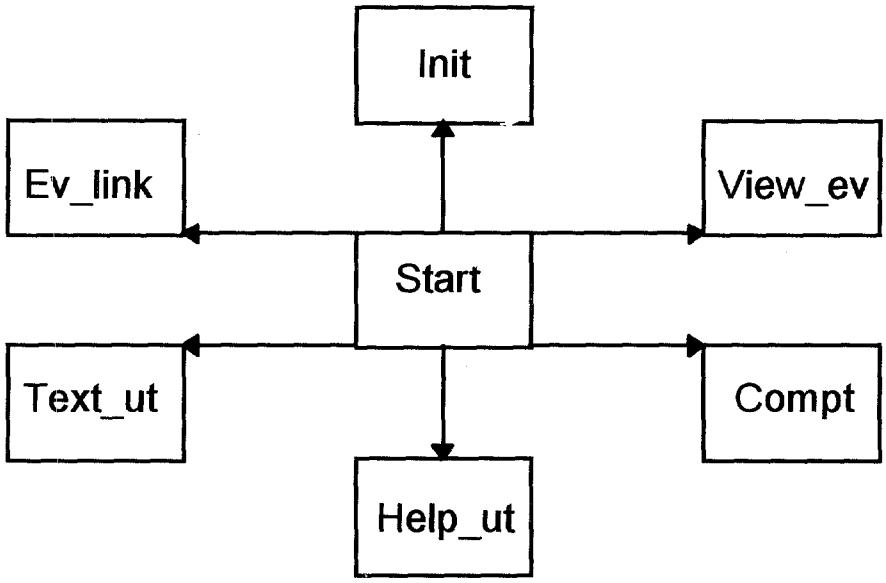

Resident part located on the workstation

Fig. 2. START program structure

Program unit EV_LINK contains procedures that maintain the interface with the "slave" workstation and issue the error and alarm messages about the system malfunctions.

The communication with the "host" workstation and set of interruptions providing the access to the informational block is maintained by the program component EV_REZID residently located on the "slave" workstation.

3.3. INFORMATIONAL FIELD STRUCTURE

The data structure includes the set of files with the informational fields of the toolkit and configurational file DUTYPORT.CNF.

The informational field structure is determined to a great extent by the above-mentioned subdivision of the water area near the protected coastal zone into four zones (and corresponding subdivision of the TWS Standard Procedure into four schemes):

zone 1 - is the near shore zone of the Pacific Ocean i.e. the North-East part of the Pacific bounded by the arc with the radius of 300 km with the center in Yuzhno-Sakhalinsk;

zone 2 – is the water area of the Sea of Japan ;

zone 3 – is the water area of the Sea of Okhotsk;

zone 4 – is the remote zone of the Pacific, defined as the part of the ocean outside the area corresponding to zone 1.

It must be noted that the tsunami waves generated by tsunamigenic earthquakes whose sources are located in the water areas corresponding to zones 1 and 4 can also appear in the Sea of Okhotsk (zone 3).

The water area (one of the above-mentioned), the corresponding warning procedure and processing algorithm are determined by the geographic coordinates of a specific earthquake.

The following data sets are associated with each zone:

- the bathymetry data (files CHEME<n>.CTD), (hereinafter n=1 - 4);
- the region mask (files CHEME<n>.MTD);
- the information about historical tsunamigenic earthquakes whose sources were in the n-th water area (CHEME<n>.EVN);
- the information about the protected points (files CHEME<n>.PNK);
- the tables of the inverse isochrone and reference tables (files <point>.TS<n>).

It is to be emphasized that only the inverse isochrones' tables of the above-listed structures can be generated directly by the software tool-kit facilities.

The output data element contains the number of the warning message dissemination scheme determined by the geographical zone of the source of the tsunamigenic earthquake, the names and geographical coordinates of the respective protected points, exected times of the tsunami arrival at these points, characteristics of the recorded earthquake and some additional official information.

3.4. ON-LINE OPERATIONS

The work of the duty oceanologist begins in the operation window of the preliminary setting where the name of the person on duty is set, the current date and time are fed or corrected. These parameters are further used for message generation and to log the events of the watch.

The basic operations including the input of the incoming information about the tsunamigenic earthquakes, the calculation of the tentative tsunami travel times, work with informational subsystem are performed from the main menu (see Fig.3.a). Shown in the results' window are the number of the corresponding warning scheme, list of the protected points and expected tsunami travel times in those points (see Fig.3.b). The on-line diagnostic window indicates the hardware malfunctions and the user error messages.

Duty oceanologist working with the main menu of the software complex gains the access to the informational subsystem. The POINTS fragment (see Fig.4) enables the user to look through the list of points falling under the Standard Regulations to some

scheme selected for the scroll and to check their geographical coordinates, to confirm or to deselect the point activity. Here it is possible also to calculate the tables of the inverse isochrones of the tsunami waves for each point in the selected water area and represent the calculated tables as charts on the display.

The interacting with the EARTHQUAKES fragment (see Fig.5) of the informational subsystem the duty oceanologist gains access to the historical data stored in the informational field. After the tentative values of the tsunami travel times are transferred to the "slave" workstation the user gains access to the submenue of the refining calculation where the direct modeling of the tsunami wave propagation is possible as well as the isochrones calculation by ray method (see Fig.6).

The times calculated at this stage can be entered into the respective informational field and transmitted to the "slave" workstation.

CONCLUSION

The presented mathematical models, numerical algorithms and software-hardware tool-kit carries out one of the fundamental TWS tasks, i.e. the determination of the tsunami travel time during tsunamigenic earthquake as well as the warning messages issue. At the same time the development of this tool-kit resulted in the concept formation which seems promising for the further automation of the TWSs and their integration into the international systems.

The possibility to extend the functions of the software is studied including the forecast program blocks predicting the dynamic characteristics of the tsunami waves, units supporting the direct interaction with the geophysical and seismic gauges and recorders, program blocks allowing for the specific hydrometeorological conditions etc.

The hardware-software tool-kit thus modified could prove the basis for the creation of the region automatic warning systems about a wide range of natural and man-made hazards.

ACKNOWLEDGMENTS

The authors are glad to acknowledge the great contribution of A. N. Sudakov and V. Yu. Kostyuk to the implementation of the algorithms and D. A. Shkuropatsky who participated in the preparation of the documentation and also express their gratitude to I. A. Zyskin and K. I. Nepop for their most valuable opinion and advice given in the course of our discussions.

REFERENCES

1. Urusov, Yu.I. Shokin: On the Modelling of the Interaction of Long Surface Water Waves with the Partly in Submerged Body}, Proceedings of the All--Union Sympo-

sium on Numerical Methods in the Wave Hydrodynamics, (Krasnoyarsk, 1991 (in Russian)), pp.33-40

2. Urusov, G.S. Khakimzyanov, Yu.I. Shokin. Numerical Study of the Surface Water Waves Run-up on the Partly Submerged Obstacles Based on the Non-linear-Dispersive Shalow-Water Model, Proceedings of the All-Union Symposium on Numerical Methods in the Wave Hydrodynamics, (Krasnoyarsk, 1991 (in Russian)), pp. 27-32
3. Kim, R.O. Reid, R.E. Whitaker: On an Open Radiational Boundary Condition for Weakly Dispersive Tsunami Waves, J. Comput. Phys., Vol. 76, pp. 327-348, (1988)
4. Flaten, O.B. Rygg: Dispersive Shallow Water Waves over a Porous Sea Bed}, Coastal Engineering, Vol. 15, pp.347-369, (1991)
5. Sudakov A.N., Filimonov V.V., Chubarov L.B. Development and installation of the software and hardware tool-kit for the automatized tsunami warning system of Sakhalin Hydrometeorological commettee tsunami centre. Report of the Krasno- yarsk Computing Center, 1990, Krasnoyarsk, (in Russian).
6. Kuzminykh I.P., Lanin Yu. F., Zyskin I.A. The development of a unified automation tsunami warning system supported by modern technical facilities. Vychislitelnyi Tekchnologii, Vol 1, No. 3, pp.75-79, 1992, Institute of Computational Technologies, Novosibirsk, (in Russian).
7. Yu.I. Shokin, L.B. Chubarov, V.A. Novikov, A.N. Sudakov. Calculation of Tsunami Travel Time Charts in the Pacific Ocean. Modeles, Algoritms, Techniques, Results, Tsunami Hazards, 1987, Vol 5, No. 2, pp.85-113.

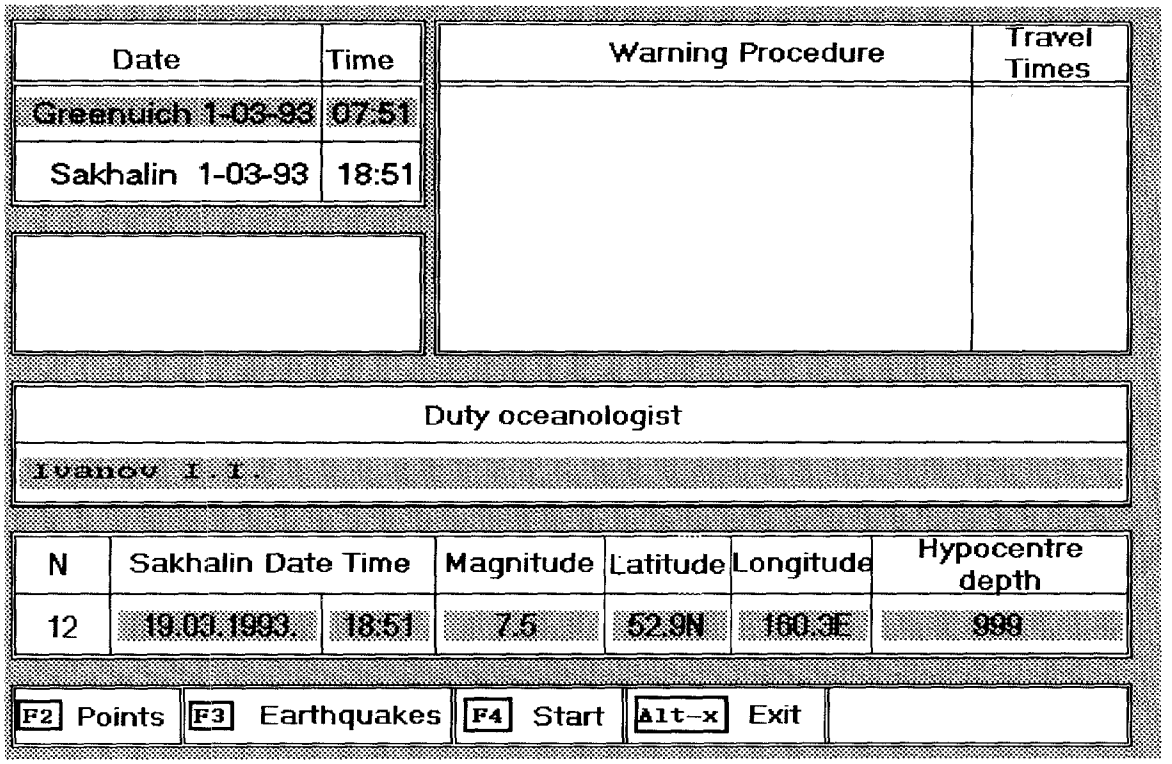

Fig. 3(a). Main dialogue box

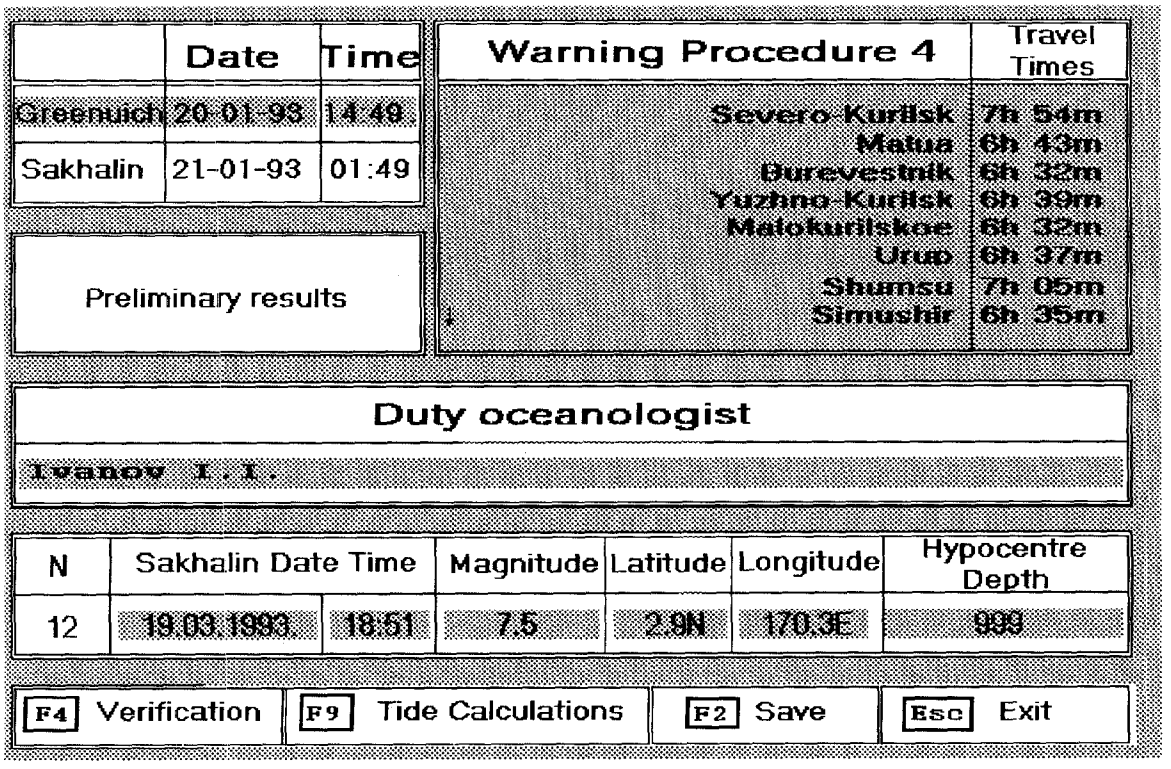

Fig. 3(b). Dialogue box:"Preliminary results"

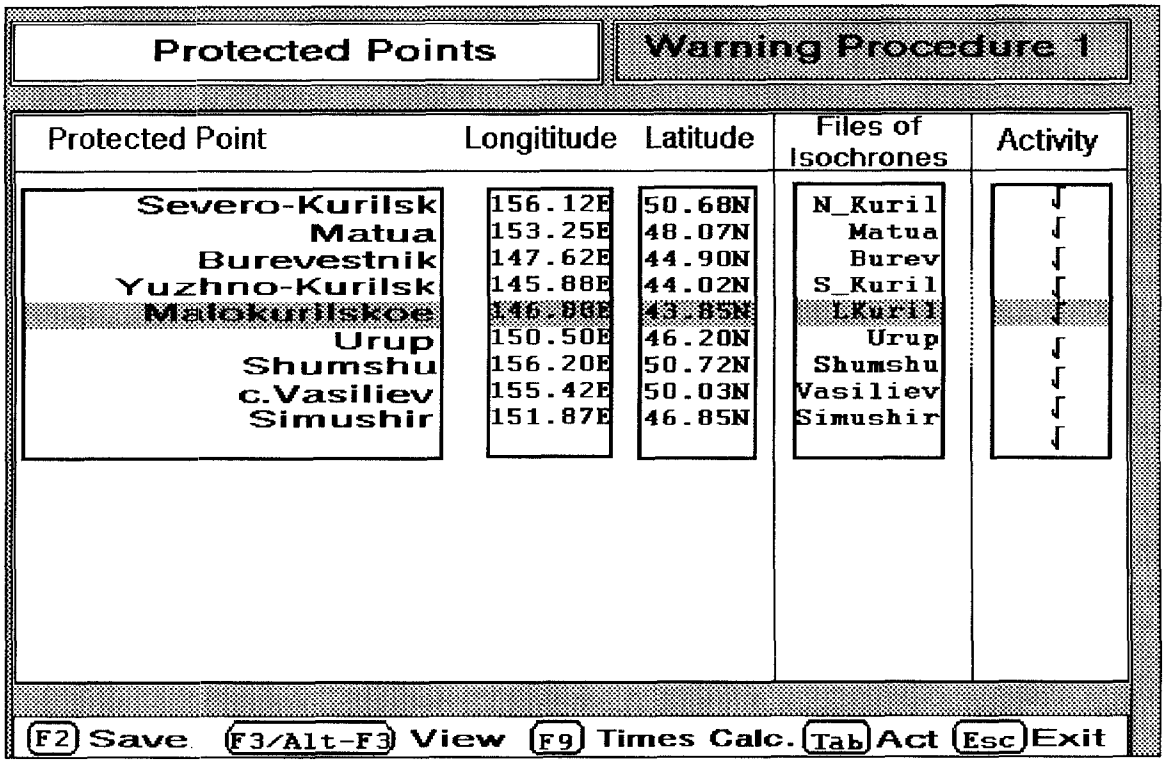

Fig. 4. Dialogue box "Points"

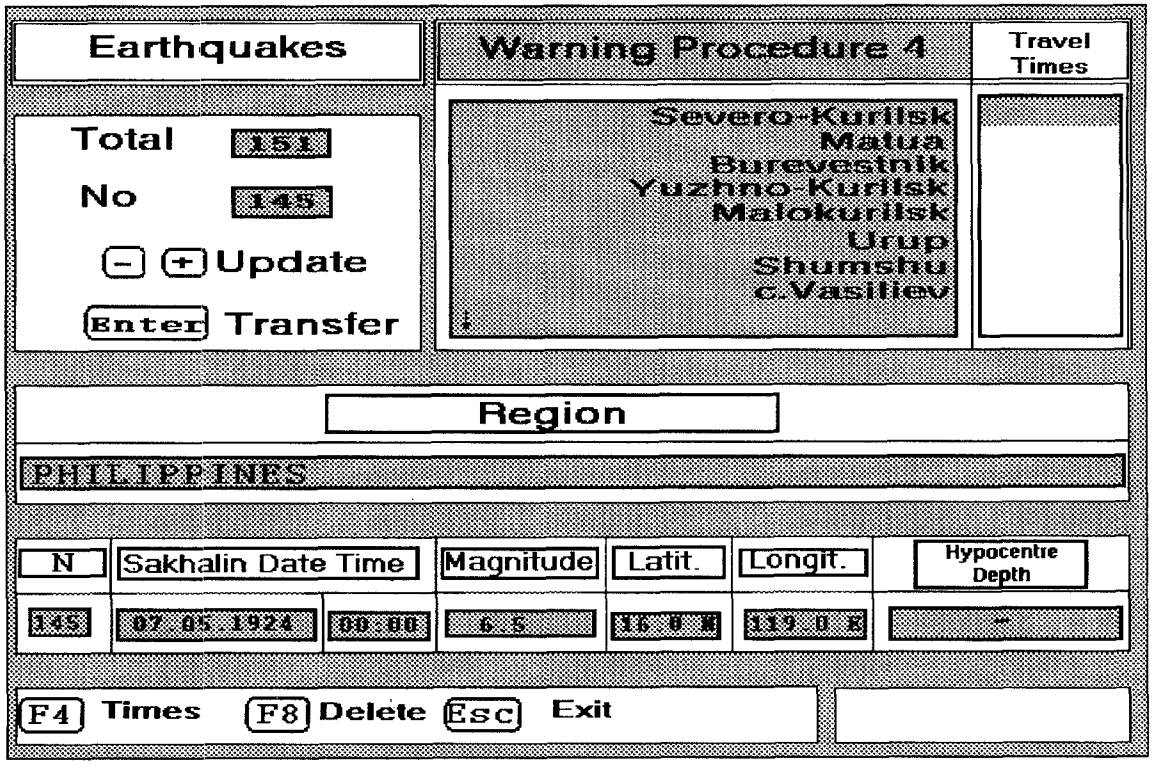

Fig. 5. Dialogue box "Earthquakes"

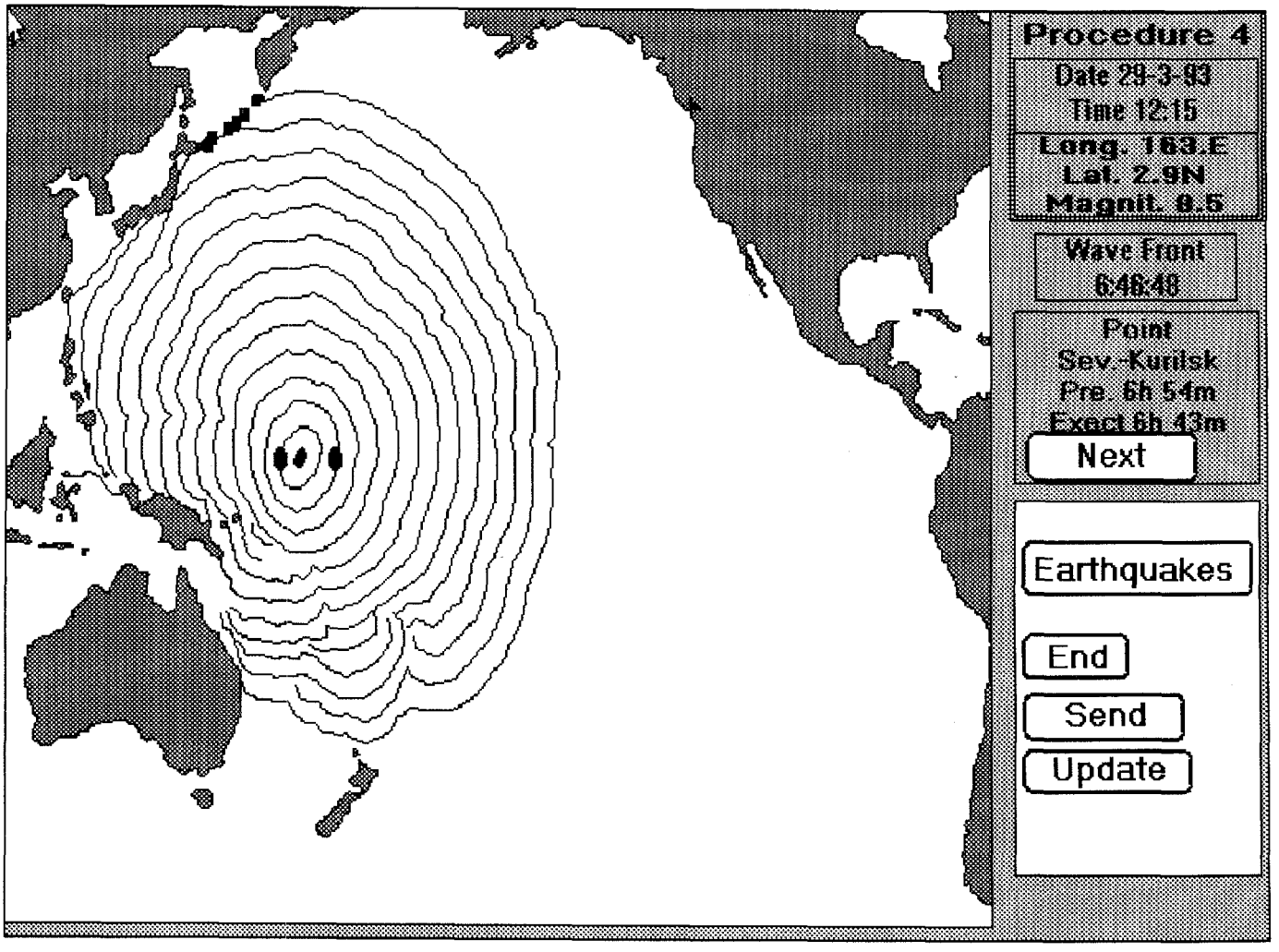

Fig. 6 Panel of the refining calculation of the tsunami traveling times

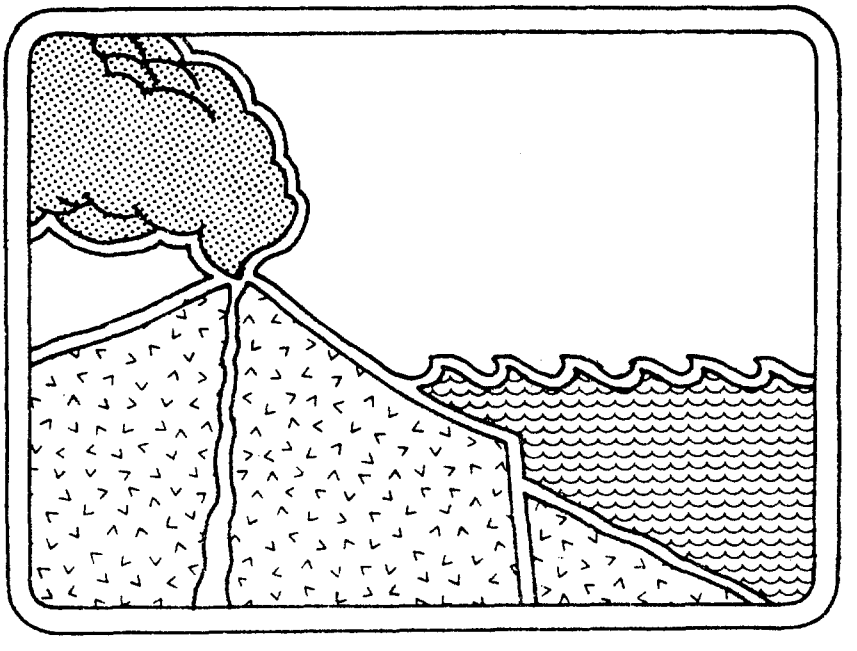

MODELING OF TSUNAMI PROPAGATION DIRECTED AT WAVE EROSION ON THE SOUTHEASTERN AUSTRALIA COAST 105,000 YEARS AGO

Anthony T. Jones
Oceanus International Consultants
1401-1166 Alberni Street
Vancouver, BC V6E 3Z3
Canada

Charles L. Mader
Mader Consulting Co.
1049 Kamehame Drive
Honolulu, HI. 96825-2860
U.S.A.

ABSTRACT

Catastrophic wave erosion on the southeastern coast of Australia has been attributed to a Hawaiian tsunami generated by the Alika 2 debris avalanche approximately 105,000 years ago. We examine the likelihood of a Hawaiian underwater mega-landslide as the tsunami source, using numerical tsunami propagation modeling, performed with the *SWAN* code which solves the non-linear long wave equations. The tsunami generation and propagation were modeled using twenty minute ETOPO5 topography for the Pacific Basin. Results for a hypothetical avalanche in the Hawaiian Islands, ten times the volume of the Alika 2 debris avalanche, show that Hawaii can not be the source for a 15 m wave on the Australian coast. An asteroid impact in the Central Pacific is examined as an alternative source for the erosional wave. Modeling results indicate that the impact of a 6 km asteroid could generate significant wave run-up along the southeastern coast of Australia.

Introduction

Wave trains generated by submarine mega-landslides off the island of Hawaii are postulated to have destroyed Australian coastal barrier dunes (reference 1). The absence of last interglacial dunes south of Newcastle along the coast of New South Wales is believed to be the result of a tsunami. Erosional evidence such as clefts, flutes, and sickle troughs in sandstone in addition to removal of 1200 m^3 of sandstone from a depression at Tura Head, New South Wales are interpreted as a result of a tsunami. At Haycock Point, 10 km south of Tura Head, Tertiary sediment capping headlands have been eroded up to an elevation of 16 m. Tsunami propagation numerical modeling was undertaken to examine the likelihood of a Hawaiian source for these erosional features.

Lanai Tsunami 105 Ka

Moore and Moore in reference 2 proposed that a giant wave or set of waves struck the Hawaiian Islands depositing marine materials at anomalously high elevations. On the island of Lanai, fragments of corals and mollusks are reported at 326 m elevation on the southern coast of the island. Neighboring islands have unusually high marine fossils in brecciated deposits. Unique gravel bedforms on Lanai have been interpreted as the result of the giant wave returning swash (reference 3).

The timing of the wave event is based on $^{230}Th/^{234}U$ dating of coral clasts collected at three sites ranging from 115 m to 155 m elevation (reference 3). The estimated date of the giant wave event is 105 ka. The giant wave event has been linked to one or more of the major submarine landslides discovered off the flanks of the Hawaiian Ridge (reference 4). At least 68 major landslides over 20 km in length have been described from GLORIA survey along the Hawaiian Island chain (reference 5). Turbidites from the mega-landslides have been recently identified from cores on the outer flank of the Hawaiian Arch, almost 340 km due west of the island of Hawaii (reference 6). In these cores, the age of the upper most volcanic sands layer, based on paleomagnetic data and biostratigraphy, is $\sim 100 \pm 20$ ka (reference 6) and is in general agreement with the estimated occurrence of the Alika 2 debris avalanche (reference 4). Recently, however, the interpretation of the 326 m material and its history of deposition has been questioned. The 326 m site on Lanai is suggested to be a remnant of a native Hawaiian foot trail cairn system (reference 7).

The Lanai tsunami has been previously modeled to determine if the identified submarine slumps and debris avalanches off Hawaii could generate a 326-m run-up on the south coast of the island of Lanai (reference 8). Estimated volumes of the submarine landslide were obtained from GLORIA sea-floor imaging (see reference 4). Modeling results indicate that only a very large Alika landslide off the Kona (west) coast of the island of Hawaii would cause the required ~400 m high run-up. For the assumed landslide model, to obtain the necessary run-up, a volume of 1600 km^2, greater than twice the likely volume of the Alika 2 debris avalanche, is required. The modelling effort was restricted by several assumptions including the simplicity of wave generated by the landslide and the instantaneous nature and size of the disturbance (see reference 9 for further discussion).

Modeling Hawaiian Tsunami Source

The generation and propagation of a Hawaiian tsunami was modeled using an ETOPO5 20 minute topographic grid for the Pacific Basin. The modeling was performed using the SWAN code (reference 10). Figure 1 shows the selected locations for determining propagating wave characteristics. The Hawaiian landslide that caused the tsunami was assumed to be ten times larger in area than the landslide that we believe occurred off the coast of Hawaii around 105 ka (reference 4). Wave propagation from this source is presented in Figure 2. The tsunami wave rapidly decays as it propagates across the Pacific Ocean. Wave characteristics at selected locations are presented in Table 1. Wave heights at selected locations are shown in Figure 3. The wave that arrives at the Australian coast is very small. While run-up from deep water could double the wave amplitude, the wave dispersion, which is not considered in the calculations, would reduce the amplitude by at least one-half or more depending upon the period of the initial wave. Therefore, the calculated results are probably upper limits for the run-up wave amplitude.

TABLE 1

Wave Characteristics for Propagated Waves

Location	Depth (m)	Mega-Landslide Amplitude Lowest (m)	Mega-Landslide Amplitude Highest (m)	Mega-Landslide Period Approx. (sec)	Asteroid Amplitude Lowest (m)	Asteroid Amplitude Highest (m)	Asteroid Period Very Approx. (sec)
1. Hawaii	4602	-200	+150	3000	-190	+190	2000
2. Australia	4530	-1	+1	4000	-20	+15	8000
3. New Zealand	2191	-4	+4	3000	-20	+40	1500
4. Solomon Islands	3005	-30	+40	1500	-100	+100	1000
5. Wake	5344	-20	+15	3000	-60	+60	1500
6. Japan	5251	-10	+10	3000	-45	+35	1500
7. California	3320	-8	+8	2000	-60	+30	2000

Notes:

Landslide (150 km, +1 km, -1 km)
Asteroid (150 km diameter cavity, 5 km deep)

Modeling Central Pacific Asteroid Impact

Given that the Hawaiian mega-landslide is an unlikely source for the NSW erosional features, we examined the likelihood of an extraterrestrial impact in the central Pacific causing the required run-up in NSW. Over the Pacific Ocean, there are annually approximately two explosive meteoric impacts in the Earth's atmosphere. Chapman and Morrison (reference 11) have calculated that within the next 100 years, the probability of a kilometer-sized object colliding with Earth is 1 in 10,000. With the Pacific Ocean representing 35% of the Earth's surface, the Pacific Ocean is a likely candidate to receive the anticipated colliding boloid. Estimated frequencies of meteorite impacts over the Pacific Ocean for scaled asteroids are one in 10,000 years for 1 km size structures, one in 100,000 years for a 5 km diameter structures and one in 50 million years for an asteroid with a diameter of 20 km.

Using a site in the central Pacific shown in Figure 1, we examined the wave propagated by an impact of an asteroid 6 km in diameter. We assume that such an asteroid would produce a water cavity approximately 150 km wide and 5 km deep. Initial water cavity size is based on similarity scaling parameters for a 10 km diameter asteroid with an impact velocity of 30 km/sec and a density of 5.0 g/cc (reference 12). A 6 km diameter asteroid is about the size of the Shoemaker-Levy 9 (Jack Hills, private communication and Johdale Solem, Los Alamos National Laboratory).

Wave propagation from the described asteroid impact in the central Pacific is presented in Figure 4. The leading wave bore is separated further from the secondary waves in this case than in the earlier example of the Hawaiian mega-landslide source (cf. Figure 2). Arrival at the NSW coastline is within 8 hours of the impact event. Figure 5 displays the wave heights from the described impact. The south coast of Australia is calculated to receive a 15-m wave, whereas Hawaii would receive a wave approaching 200 m. Numerical calculations indicate that an asteroid about the size of the recent Shoemaker-Levy 9 could result in large waves required for both the Lanai and Australian coast. Clearly, smaller asteroids nearer Australia could generate run up of 15 m along the New South Wales coast.

Discussion

There are several possible sources for the Australian erosional event. Besides asteroid impacts, tsunamigenic earthquakes along the subducting Tonga-Kermadec arc and submarine landslides off New Zealand could generate a source for the southeastern coast of Australia. Seismic activity along the Tongo Kermac Trench could have generated waves. This stretch of the plate boundaries has been fairly active in historic times (reference 13). However, whereas earthquakes partition approximately 1 to 10 % of their energy into water waves (reference 14), impact events potentially yield more intense tsunamis due to larger energies involved in planetary collision.

Submarine landslides possibly triggered by earthquakes could have also generated waves of sufficient energy to cause localized erosion along the NSW coast. However, one should expect to observe turbidity flows and slumps as well as evidence of tsunami deposits on the shores of New Zealand which so far has not been reported.

In conclusion, our numerical analysis of tsunami propagation from a Hawaiian mega-landslide indicate that the landslide-based tsunami would not generate a 15 m wave along the southeastern coast of Australia. Alternatively, an impact from an asteroid in the central Pacific could generate a wave along the coast of New South Wales that meets the requirements of the erosional features identified by Young and Bryant (reference 1). Whether there is further geological evidence supporting an asteroid impact in the central Pacific within the timeframe required for the New South Wales erosional event remains to be investigated.

Acknowledgments

The authors gratefully acknowledge the contribution of K.A.W. Crook (University of Hawaii), Jack Hills and Johdale Solem (Los Alamos National Laboratory), Pat Wilde (Office of Naval Research) and Mary Hunt (Lawrence Berkeley Laboratory).

References

1. R. W. Young and E. A. Bryant, "Catastrophic wave erosion on the southeastern coast of Australia: Impact of the Lanai tsunamis ca. 105 ka?" Geology, Vol. 20, 199-202 (1992).
2. James G. Moore and George W. Moore, "Deposit from a giant wave on the Island of Lanai, Hawaii," Science, Vol. 226, 1312-1315 (1984).
3. George W. Moore and James G. Moore, "Large scale bedforms in boulder gravel produced by giant waves in Hawaii," Geological Society of America Special Publication No. 229, pp. 101-110 (1988).
4. James G. Moore, David A. Clague, Robin T. Holcomb, Peter W. Lipman, William R. Normark, and Mark E. Torresan, "Prodigious submarine landslides on the Hawaiian Ridge," Journal of Geophysical Research, Vol. 94, 17,465-17,484 (1989).
5. James G. Moore, William R. Normark, and Robin T. Holcomb, "Giant Hawaiian Landslides," Annual Review of Earth and Planetary Science, Vol. 22, 119-144 (1994).
6. Michael O. Garcia and Donna Meyerhoff Hull, "Turbidites from giant Hawaiian landslides: Results from Ocean Drilling Program Site 842," Geology, Vol. 22, 159-162 (1994).
7. Anthony T. Jones, "Elevated fossil coral deposits in the Hawaiian Islands: a measure of island uplift in the Quaternary," Ph.D. dissertation, University of Hawaii, (1993).
8. Carl Johnson and Charles L. Mader, "Modeling the 105 Ka Lanai Tsunami," Science of Tsunami Hazards, Vol. 11, 33-38 (1994).
9. Paul H. LeBond and Anthony T. Jones, "Underwater landslides are less effective than abrupt shifts in sea bottom at producing tsunamis," Science of Tsunami Hazards (1995).
10. Charles L. Mader, *Numerical Modeling of Water Waves*, University of California Press, Berkeley, California (1988).
11. Clark R. Chapman and David Morrison, "Impacts on the Earth by asteroids and comets: assessing the hazard," Nature, Vol. 367, 33-40 (1994).
12. Thomas J. Ahrens and John D. O'Keefe, "Impact of an asteroid or comet in the ocean and extinction of terestrial life," Journal of Geophysical Research, Vol. 88, Supplement A799-A806 (1983).
13. S.L. Soloviev, "Recurrence of Tsunamis in the Pacific," In: *Tsunamis in the Pacific Ocean*, East-West Center Press, Hawaii, pp. 149-163 (1970).
14. Robert L. Weigel, "Tsunamis," In: *Earthquake Engineering*. Prentice Hall, New Jersey, pp. 253-306 (1970).

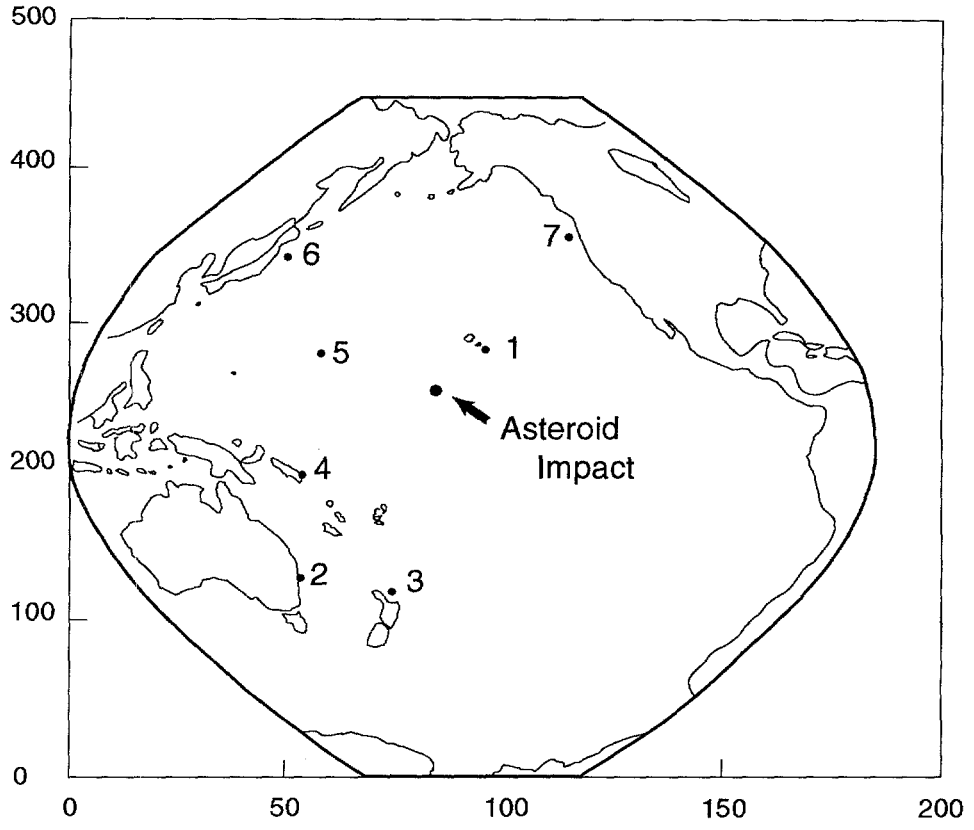

Figure 1. Location map of selected sites for tsunami propagation. Location of modeled hypothetical asteroid impact in the central Pacific is also indicated.

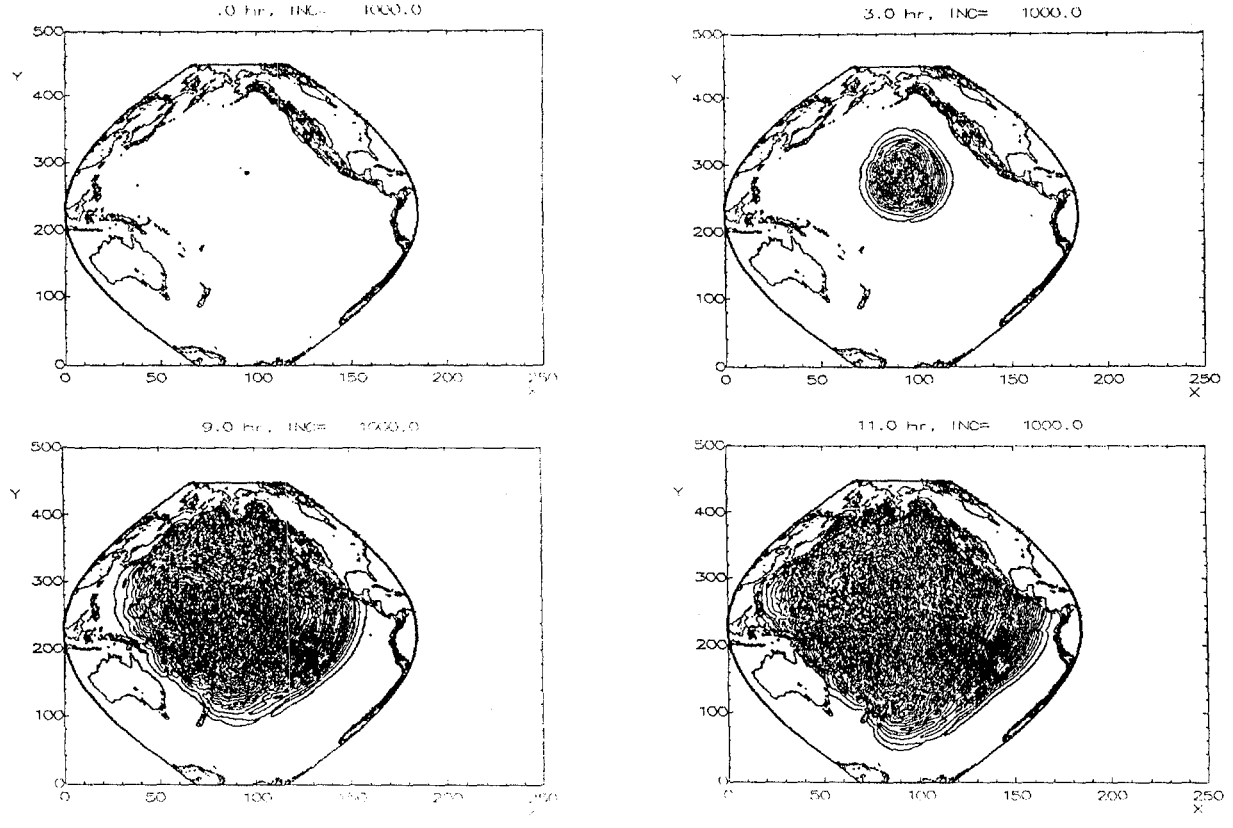

Figure 2. Tsunami wave propagation from Hawaiian underwater landslide source.

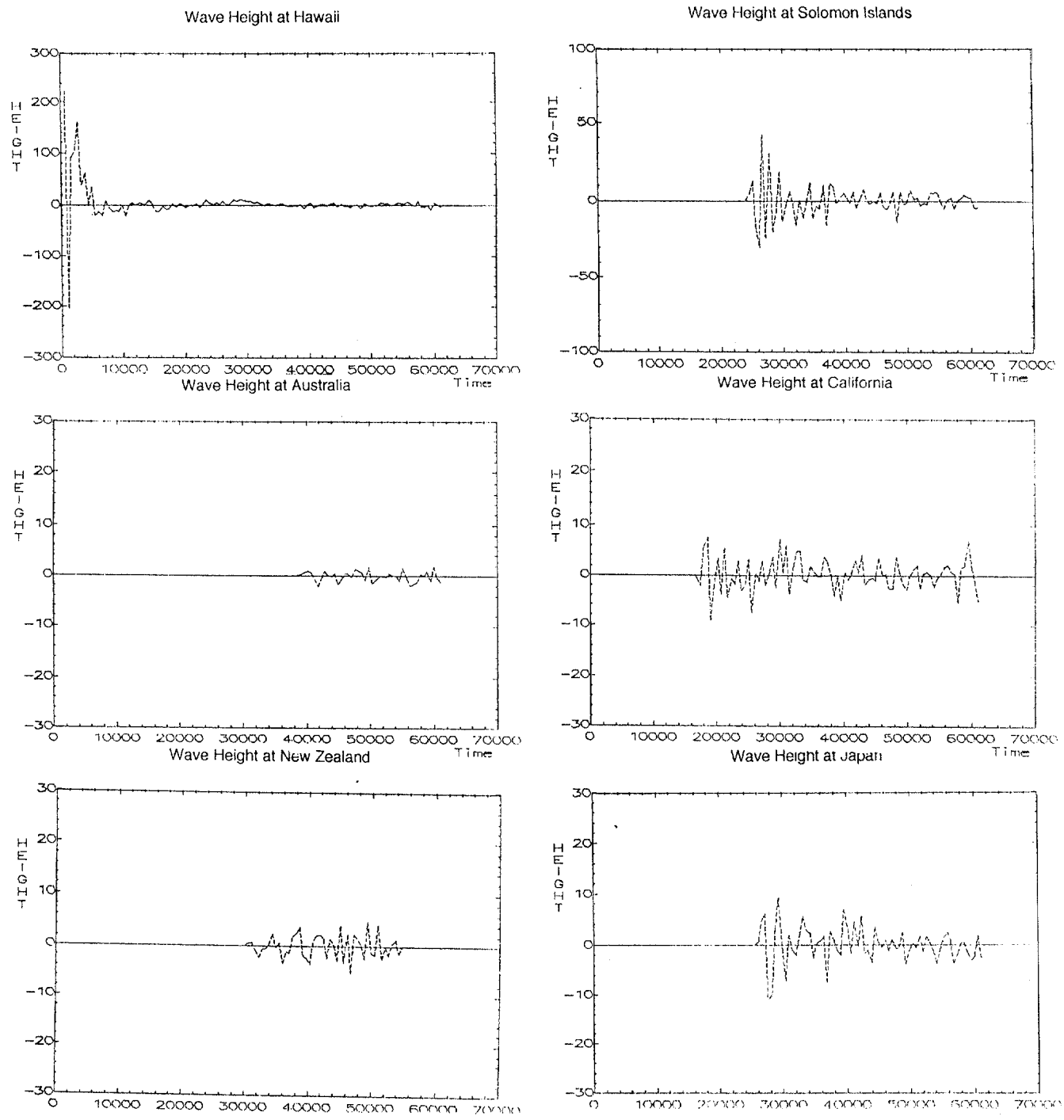

Figure 3. Calculated wave heights at selected locations for Hawaiian underwater landslide source.

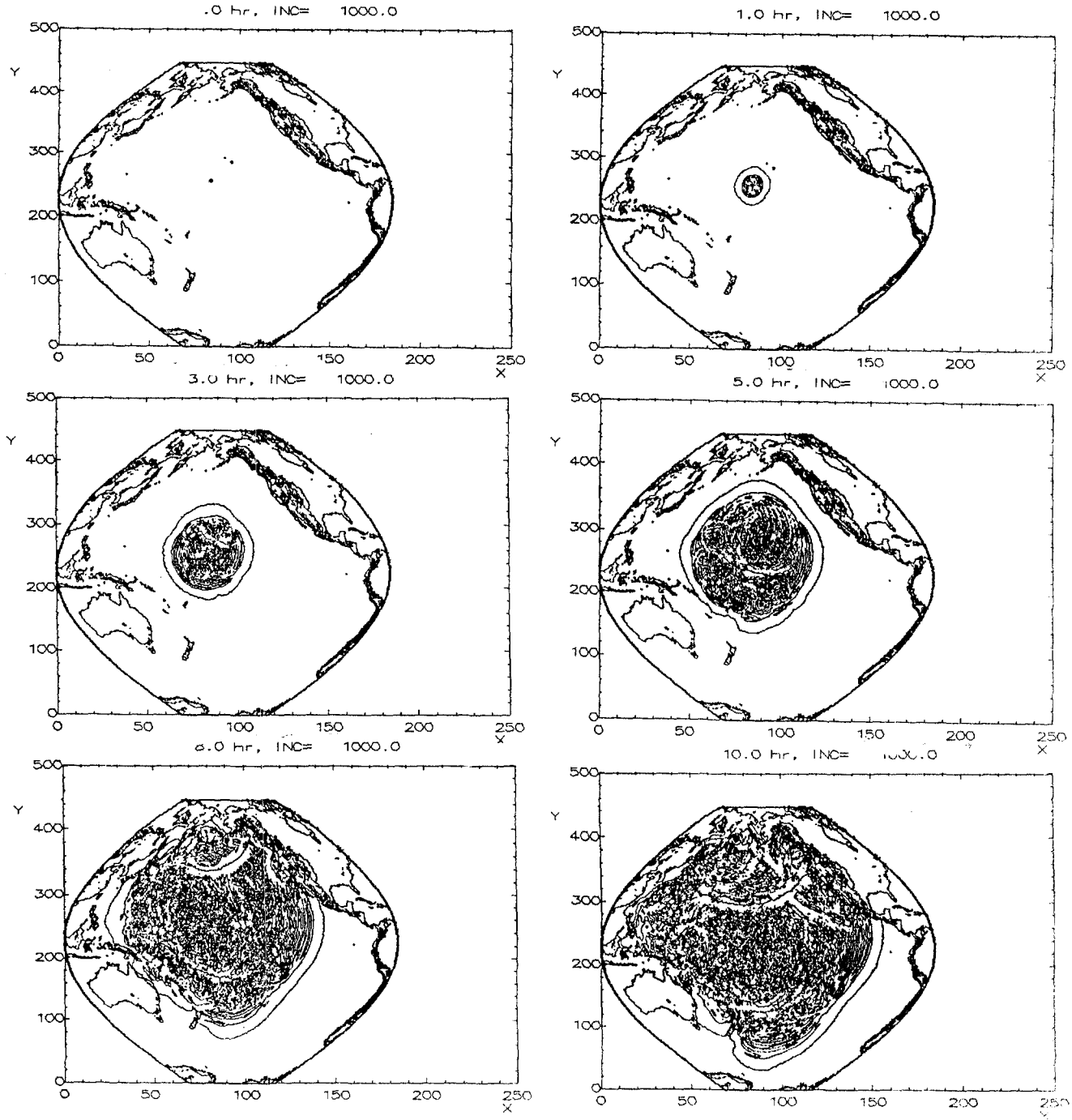

Figure 4. Tsunami wave propagation from Central Pacific asteroid impact source.

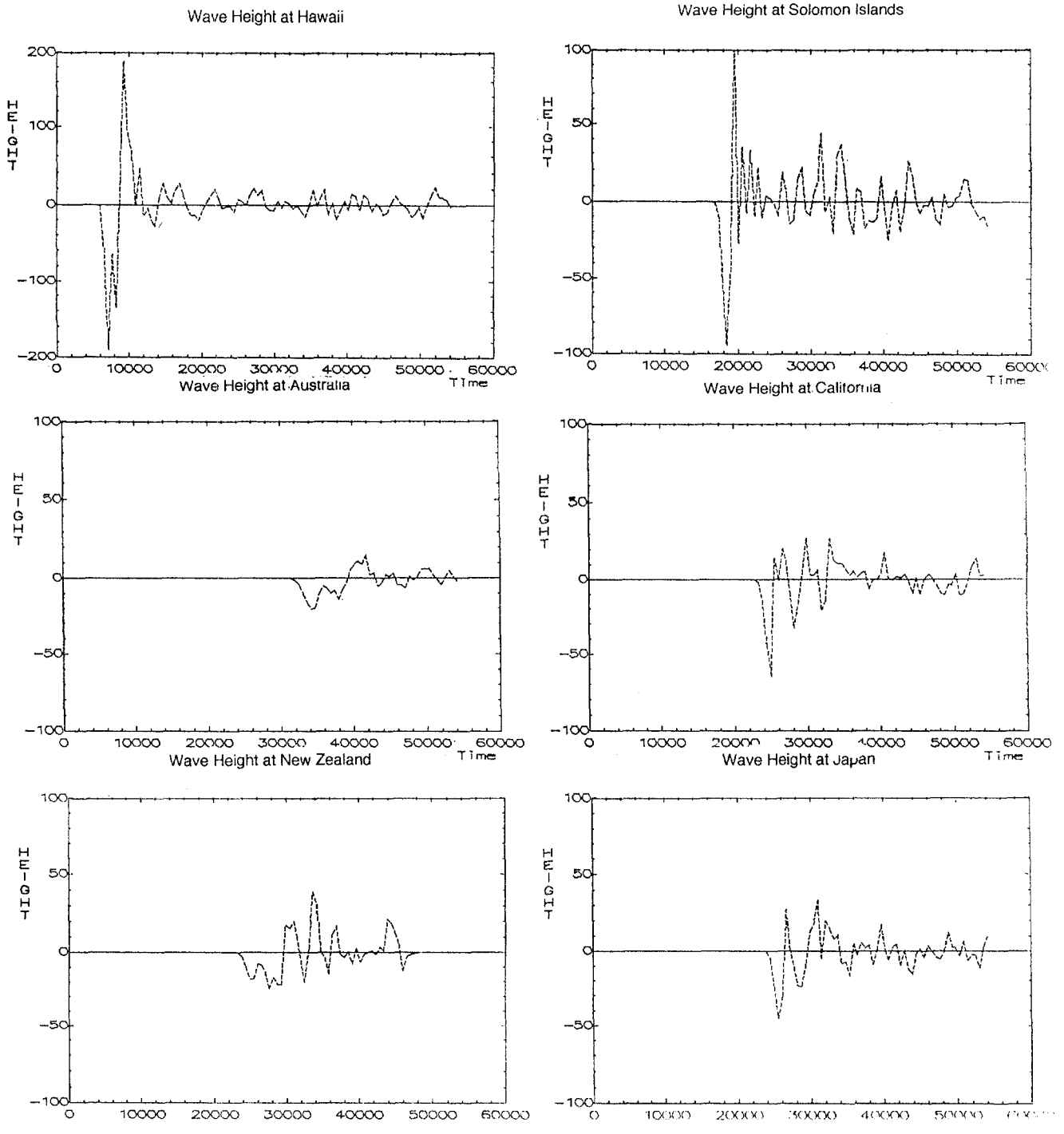

Figure 5. Calculated wave heights at selected locations for Central Pacific asteroid impact source.

OCEANIC SUBSURFACE THERMAL VARIATIONS DURING THE 1995 HYOGO SOUTH EARTHQUAKE

Shigehisa Nakamura
Shirahama Oceanographic Observatory
DPRI, Kyoto University at Kakada
Shirahama 649-22, Japan

ABSTRACT

Subsurface thermal variations of the sea water were observed before and during the 1995 Hyogo South earthquake, which occurred in the early morning of January 17, 1995. The earthquake was destructive in an area around a newly formed seismic fault line which extended from downtown Kobe to the neighbouring cities and towns. Heavy damage occurred astride the fault line on land. The epicenter of the earthquake was under the urban area of Kobe. The sea water temperature was measured at an offshore station at 2.5, 5 and 10 meters under the sea surface. Subsurface ocean thermal variation measurements could be useful to the tsunami warning system.

INTRODUCTION

An earthquake occurred around 5:45 JST in Kobe, Japan. It was destructive in both the downtown and urban area along a newly formed seismic fault which is parallel to the coast line.

Subsurface thermal variation were observed at an offshore town station mounted on a ridge off the coast facing the northwestern Pacific Ocean. The tower station was about 100 km from the epicenter of the earthquake.

The damage on land just south of the newly formed seismic fault line was severe. In this note, we concentrate only on the subsurface thermal variations observed before and during the earthquake. These variations may be closely related to the main earthquake shock.

EPICENTER and OFFSHORE TOWER

The location of the epicenter is shown in Figure 1 as a cross with the mark F. Seismic faults wee found to extend from the mark F to a line extending ENE along the coast and to a line extending SSW.

The epicenter location was initially estimated to be in the Akashi Strait, so a tsunami was expected. Several tide stations recorded the tsunami though no hazardous sea level variations were seen. The observed maximum tsunami height was about 20 cm.

The maximum acceleration of the ground motion at the Kobe Marine Observatory was 818 gal for the NS component, 617 gal for the EW component and 332 gal for the up/down component.

The Japan Meteorological Agency's estimated magnitude was 7.6 and the depth was 20 km.

An offshore tower was located as shown in Figure 1 and marked with a T. This tower was established in 1993 for the oceanographic observation of hazards around and in the coastal zones of the northwestern Pacific Ocean.

THERMAL VARIATIONS

At 5:46 JST, the Television informed us that a hazardous earthquake was occurring though no details were available. Before the message, the author who was in the Observatory was awaken by a strange P wave shock and a big S wave shock. Judging from the P and S times of the earthquake, the author estimated that the epicenter of the shocks must be at a distance of several tens of kilometers.

On the next day, the observed subsurface variations of the sea water temperatures were printed out and we observed strange variations just before and after the shocks.

In Figure 2, a part of the thermal variations is shown as water temperature variations at depths of 2.5, 5 and 10 meters at the offshore tower. This illustrates that a thermal variation may be closely related to a hazardous earthquake.

The thermal variations at 10 meter depth at the offshore tower had already started at 5:30 JST. At 10 meter depth, the water temperature started to lower uniformly with time by 5:50 JST. After the variations at 10 meter depth was seen, successively the thermal variations were found at the 5 and 2.5 meter depths. The patterns of thermal at the three depths were not similar to each other.

Minor tsunamis were found on the marigrams at 30 km west and south from the epicenter. A similar thermal variation was found to be recorded at a station 30 km south of the epicenter.

DISCUSSION

For more than 100 years, tsunami scientific research has concentrated on evaluating the maximum height of the water on the coast. The author has attempted to clarify the reference level in an area where the tectonic variations are contaminated by the existing oceanic conditions (Nakamura, 1990; 1994; 1995). It is well understood that the horizontal water motion can be significant even when the vertical water motion is not significant. We need to observe the horizontal water motion caused by any tsunamigenic earthquake. The author has noted the extent of the sea water motions during the 1995 Hyogo South earthquake (Nakamura, 1995). In the case of trans-Pacific tsunamis, a thermal variation might accompany the sea level variation (see for example, Nakamura, 1992).

The subsurface ocean thermal variations could be useful to the tsunami warning system and the existing coastal protection works.

REFERENCES

1. Nakamura S. (1990), "Secular Upheaval of Datum Levels in Relation to Tsunamigenic Earthquakes," Marine Geodesy, Vol. 14.
2. Nakamura, S. (1992), "The 1985 Chilean Tsunami around Osaka Bay," La mer, Tome 30.
3. Nakamura, S. (1994), "Annual Mean Sea Level and Tsunamigenic Earthquake in the Northwestern Pacific," Proc. International Symposium on Marine Positioning and Mapping, Hannover.
4. Nakamura, S. (1995), "Extent of Sea Water Motions at the Hyogo South Earthquake," EOS (Trans. AGU) 1995 Spring Meeting.
5. Nakamura, S. (1995), "On Annual Mean Sea Level to Upheaval of Datum Level," XII General Assembly IASPO, Hawaii, PS-05.

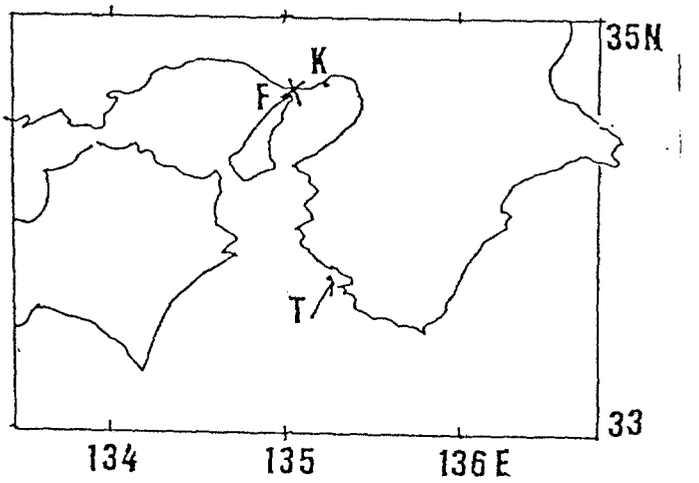

Figure 1. Geographic Locations of the Epicenter (X and F), Kobe (K), and the offshore tower station (T).

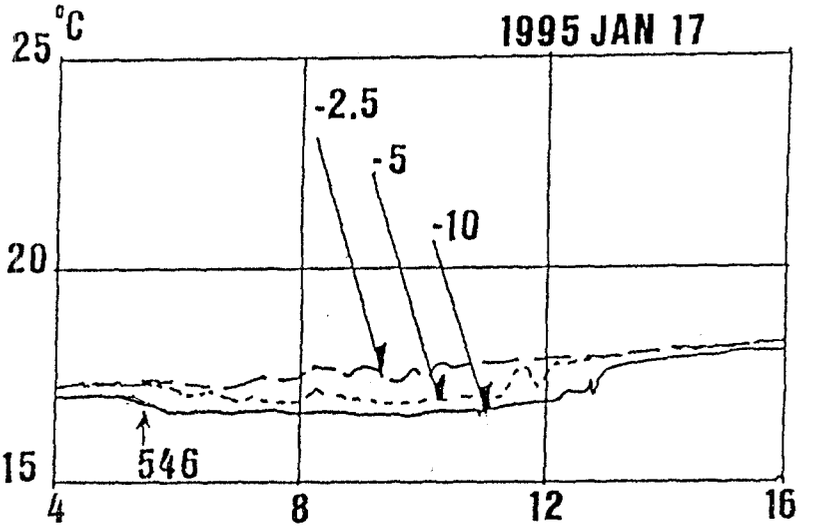

Figure 2. Thermal Variations at the Offshore Tower Station. Sea Water Temperature Variations at depths of 1.5, 5.0 and 10 meters under the sea surface between 4:00 to 16:00 JST on January 17, 1995.

NEWS BRIEFS

RESPONSE ACTIONS FOLLOWING THE CHILEAN TSUNAMI OF JULY 30, 1995

In Hawaii and Tahiti

On July 30, 1995 at 05h 11m GMT (July 29, 19h 11m LT, in both Hawaii and French Polynesia, an earthquake of magnitude Ms 8.3 occurred at 23.4 S, 70.1 W, just offshore from the city of Antofagasta in northern Chile. Because of the magnitude, the Pacific Tsunami Warning Center (PTWC) located in Ewa Beach, Hawaii, issued a tsunami warning for those within a three hour tsunami travel time from when the warning was issued and a tsunami watch for those outside of the warning area but within a six hour tsunami travel time.

Coincidentally at that time the International Coordinating Group for the Tsunami Warning System in the Pacific was wrapping up its regular biennial meeting, held this year on Tahiti in French Polynesia. The emergency management officials from various nations in the Pacific, who are responsible for tsunami warnings, were preparing to return home. When notified by the Laboratorie d'Geophysique (LDG) that a great earthquake had occurred near Antofagasta, one of the delegates from Chile, Hugo Gorziglia, immediately called his office in Valparaiso to inquire about the damage situation. The response was that although earthquake damage was widespread, tsunami run-up amounted to a few meters at most and that damage from tsunami was insignificant. Based on this information, and water level measurements from stations near the epicenter, the PTWC canceled the warning and watch a little over an hour after they were issued.

Also by coincidence the weekly flight between Papeete and Honolulu was scheduled to leave at 00h 30m, just over five hours after the earthquake. This allowed Michael Blackford, Geophysicist-in-Charge, and Charles McCreery, seismologist, at the PTWC to be in Honolulu in time for the tsunami arrival. The tsunami travel time between northern Chile and the Hawaiian Islands is about fourteen hours.

Even though Blackford and McCreery were aware that a minor tsunami had occurred in the near-source area and that the tsunami warning and watch had been canceled hours earlier, they nevertheless hastened to Ewa Beach, after clearing customs at Honolulu International Airport, to observe the tsunami's possible sweep across the Hawaiian water level gauges. They arrived about forty-five minutes before the estimated arrival at Hilo, 09h 00m LT, and reviewed the material accumulated on the event the previous evening. While they were examining the mareograms from Chilean stations, at 08h 45m LT, they received an urgent facsimile message from Francois Schindele, director of LDG, indicating that in a harbor on the island of Hiva Oe in the Marquesas Archipelago the tsunami wave height was observed to be about two meters and that some boats were swamped and sank in an eddy behind a breakwater. This was significant damage at a great distance from the source area!

PTWC immediately apprised the Office of Civil Defence of the State of Hawaii of the situation. The timing was most uncomfortable as this came only a few minutes

In the numerical model, the source was 3 cells wide (100 km) and 6 cells long (230 km) with the southwest corner at 27° S and 71.6° W. The initial upward displacement was taken as 10 meters.

The calculated maximum heights in deep water near tide gage locations are given in the following table. The numbers are all in meters.

LOCATION	DEPTH (m)	CALCULATED MAX HEIGHT	TIDE GAUGE DOUBLE AMP
Caldera, Chile	4400	0.5	1.3
Papeete, Tahiti	3515	0.2	0.15
Nuku Hiva, Marquesas	4108	0.5	1.15
Hilo, Hawaii	4399	0.1	0.85
Honolulu, Hawaii	5668	0.02	0.18
Crescent City, Calif	2201	0.12	0.35
Kesennuma, Japan	5251	0.1	0.3 - 0.4

From the calculations it is clear that in the far field, the highest amplitude (0.5 m) in the deep ocean developed in the vicinity of the Marquesas Archipelago, and that to the north near the Hawaiian Islands, the wave height (0.1 m) had diminished significantly. The wave height near Japan agrees well with tide gage records.

Although this exercise was a hindsight project, it does demonstrate that numerical simulation mirrors tsunami propagation. If this numerical simulation were available in real time during the tsunami watch, the damage in the Marquesas would not have caused apprehension to the emergency management officials in Hawaii. The question naturally arises: can numerical simulation be used in real time?

The answer hinges on the availability of a fast computer with proper software and whether knowledgeable persons can be on hand to compile source parameters and enter them into the computer. At the present time discussions are being held to install the SWAN code into the High Performance Computer on the island of Maui, Hawaii, for tsunami forecast purposes. Tailoring the SWAN code to be compatible with the High Performance Computer and administrative details on access to the computer in real time will take some time to work out. Perhaps, when forecasting with numerical simulation becomes on-line, the difficulties encountered in Marquesas, Hawaii and Japan need not recur.

References

1. C. L. Mader and G. Curtis, 1991. Modeling Hilo, Hawaii, Tsunami Inundation. *Science of Tsunami Hazards, vol. 9, 85-94.*

2. C. L. Mader, 1988. *Numerical Modeling of Water Waves.* Univ. Cal. Press, Berkeley.

3. T. Monfret et al., 1995. The July 30, 1995 Antofagasta Earthquake: an "Hypocritical" Seismic Event. *EOS* Nov 7, 1995 p F427.

before the expected arrival of the first crest at Hilo Bay, Hawaii. The consensus of the officials at federal, state, and county levels in Hawaii was to wait out the situation because, in addition to the reports from the source area of a relatively minor tsunami, Schindele also reported a minor tsunami of only twenty-five centimeters at Papeete, Tahiti. The observation of a two meter tsunami on Hiva Oe appeared to be an anomaly rather than the norm. When the tsunami did arrive in Hilo Bay, the tide gauge in the harbor registered a maximum double amplitude of 0.80m. The water level in the harbor was observed to rise and fall but no damage occurred.

In Japan

In Japan the tsunami caused an unusual stir. Augustine Furumoto happened to be in Tokyo on a business trip on July 31, 1995. Reading the evening edition of the Mainichi Shinbun, largest circulation newspaper in Japan, he was jerked to attention by an article in the front page that headlined "The Japan Meteorological Agency issued a tsunami warning two hours after tsunami arrival." The article was not sharply critical of the Japan Meteorological Agency (JMA); a reader got the impression that this was a report of an example of human folly that can easily happen.

We speculate on what happened in Japan. The Tsunami Section of JMA in Tokyo was keeping a watch on the tsunami sweeping across the ocean. There was no indication from near source reports and reports from Hawaii that this tsunami posed any danger. But when the tsunami arrived in Japan, some tide gages, including the one at Kesennuma and Hachinohe, registered a double amplitude of 30 centimeters. When the Tsunami Section staff noticed the 30 cm amplitude, they became apprehensive that the second and third crests could be potentially damaging. So, a low level tsunami warning was issued, according to standard operating procedures. But even with state-of-the art communication system, there is a time delay as data are transmitted in spurts; analysis and decision making consume time; and broadcasting of warning also chalks up time as messages must be routed through the news media. By the time the warning got out to the coastal areas, it was already two hours after the arrival of the first crest.

Post-tsunami Numerical Analysis

Charles Mader modeled the tsunami using the technique that successfully reproduced numerically the Chile tsunami of May 23, 1960 (cf. Reference 1). The model used a 20 minute grid of the Pacific Ocean from 110° E to 65° W and 75° S to 75° N of 555 by 450 cells. The SWAN code was used to solve non-linear shallow water equations as described in Reference 2.

The tsunami source parameters were compiled by A. Furumoto. PTWC had determined the epicenter, as given above. LDG calculated the seismic moment to be 2.3×10^{21} N-m. The rupture had proceeded southward from the epicenter (Reference 3). From the seismic moment the length of the rupture area was estimated to be 235 km, its width was assumed to be 100 km, roughly the distance from the Chilean shore to the subduction trench. The rupture area was taken to be a rectangle in the north-south direction, with the northeast corner at the epicenter.

a special message
for teachers and students

THE STORY OF

Laupahoehoe

Laupahoehoe is a low–lying peninsula north of Hilo along the Hamakua Coast. On April 1, 1946 the war in the Pacific had ended just seven months earlier, and people were beginning to feel better about the future. There probably had been so many bad things in the past to think about that it was difficult to remember earlier tragedies caused by tsunamis. After all, a generation of students and teachers had passed through Laupahoehoe School since anyone had been killed in Hawai'i by a tsunami.

On April 1, 1946 the students of Laupahoehoe had only two more months until summer vacation. However, many of those students and their teachers would not live to see even the next day, let alone other school years and lifetimes of summers to come. Had they known a few simple facts about tsunamis, their lives might not have ended on that horrible day.

Too bad the teachers didn't know about tsunamis. Too bad they hadn't told their students some simple facts like:

- tsunamis are dangerous;
- the first wave is not always the largest;
- sometimes the first indication of a tsunami is the disappearance of water; and,
- tsunamis can move faster than a person can run.

Such simple knowledge could have saved their lives. Why? Because on April 1, 1946 the first wave at Laupahoehoe was small, and some of the teachers and students saw it! Others noticed an unusual disappearance of water, exposing the ocean floor.

Unfortunately, the students and teachers did not understand the deadly implications of what they saw. The necessary formal education, scientific knowledge, or traditional knowledge of the sea was either non–existent or failed to emerge in the few remaining minutes that they had left to save their lives. As a result five teachers and 16 students were swept to their deaths. Elsewhere in Hawai'i an additional 138 people lost their lives in the 1946 tsunami.

A similar disaster occurred again in 1960 when a tsunami from Chile killed 61 people in Hilo. This happened in spite of adequate warnings provided by the Pacific Tsunami Warning Center. The possibility of a repetition of these tragedies is increased by the tremendous growth in the past 30 years and the fact that we now have a second generation of children in our schools who know little about tsunamis. (From 1900 through 1964, eight Pacific–wide tsunamis with heights of 10 feet or more above sea–level struck low–lying areas of the state. Five had heights of 20 feet or more, four were 30 feet or more, and two were 50 feet or more. From 1965 through 1994, no large Pacific–wide tsunamis have struck Hawai'i.)

The quiet period of recent years will not continue indefinitely. Large tsunamis will once again strike Hawai'i. Children and adults need to take tsunami warnings seriously, and they need to know the signs of tsunamis in case sirens are defective, or they are in remote or noisy areas where sirens can't be heard.

Also, there may exist many dangerous misconceptions about tsunamis. Do people know that:

- all major coastal areas of the state have been struck by large tsunamis;
- some of the largest tsunamis from earthquakes originating in the North Pacific may be found on the northern shores of O'ahu and Kaua'i, rather than in Hilo;
- large locally generated tsunamis occurred in 1868 and 1975 with heights as great as 40 feet;
- four other locally generated tsunamis occurred in this century; and,
- tsunamis have killed 221 people in Hawai'i during this century compared to seven deaths due to hurricanes?

Major tsunamis are inevitable. A few minutes of classroom instruction a year will eventually save the lives of our students, their friends, and their relatives. With the help of teachers throughout the state, the tragedy of Laupahoehoe need not be repeated.

When the next major tsunami strikes Hawai'i, attention will once again focus on the destructive power of nature in Hawai'i; but, hopefully, we will be able to have some consolation in the fact that we did what we could to minimize injuries and the loss of life.

The Tsunami Memorial Institute (TMI) is dedicated to informing teachers of tsunami hazards and providing them with necessary educational materials. These materials can also serve as an introduction to regular instruction regarding natural hazards and such Earth science topics as earthquakes, volcanoes, ocean waves, and plate tectonics. **Free information on TMI educational products for all grade levels will be provided on request.** (The nature and costs of these products are respectful of the workloads and responsibilities imposed upon teachers, their resulting time constraints on new initiatives, and the limited budgets of educational organizations.)

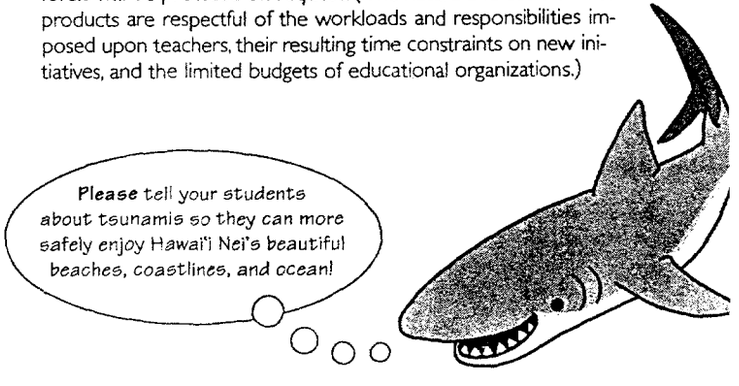

This elemental knowledge could prevent injuries and save many lives. More time and effort in discussions of definitions, scientific concepts, and historical data using other resources may expand a student's level of understanding from mere awareness of elemental concepts to knowledge of fundamental principles and observations. The following are additional resources which may be useful for that purpose.

Dudley, W. and M. Lee, 1988. *Tsunami!*, University of Hawai'i Press, Honolulu, Hawai'i, 132 pp.

Contains personal recollections of tsunamis in Hawai'i, especially in the Hilo area. Available in most bookstores or from the University of Hawai'i Press.

Walker, D. A., 1994, *Tsunami Facts*, SOEST Report 94–03.

Contains data (tables and maps) in meters and feet on all reported tsunamis in Hawai'i. Also has listings of "Tsunami Facts", "What You Should Do", and a "Self-Quiz". Maps of runups can be used to personalize the importance of tsunami awareness for differing islands or particular coasts of islands. Useful as a teacher's source book. The "Self-Quiz" is appropriate for intermediate and high-school students. Copying of this text, or portions of it, is permitted and encouraged. Available at no charge to school libraries throughout the State.

Walker, D. A., 1994, *Tsunamis in Hawai'i*, Tsunami Memorial Institute, one sheet.

A 2'x 3' color poster which can serve as a classroom focal point for tsunami awareness and education. Contains maps, definitions, "What You Should Know", and "What You Should Do".

Other resources are available from the International Tsunami Information Center in Honolulu. (Telephone: 808-541-1658)

For more information about TMI publications write to:

Dr. Daniel A. Walker
Tsunami Memorial Institute
59-530 Pupukea Road
Haleiwa, Hawai'i 96712

TMI Publication No. 02

'Iliki ke kai i ka 'ope'ope la, lilo;
i lilo no he hawawā.

Literal translation
The sea snatches the bundle, it is gone;
it goes when one is not watchful.

Interpretation
A person who fails to watch out often loses.
Never turn your back on the sea.

ANNOUNCEMENTS

(This page of announcemnts of coming conferences, meetings, workshops, etc. is provided as a public service to the tsunami community.)

NATIONAL DISASTER MEDICAL SYSTEM

The 1996 National Disaster Medical System (NDMS) will be held in San Diego, California, March 16-21, 1996. For additional information, contact:

NDMS
5600 Fishers Lane, Room 4-81
Rockville, MD 20857
(800) USA-NDMS. extension 444.

TSUNAMI CONFERENCE and MUSEUM INAUGURATION

April 1-2, 1996 - Hilo, Hawaii

Marking the 50th anniversary of the 1946 tsunami at Hilo, which led to the present Pacific-wide warning system, increased tsunami research, and the Centennial of the great Sanriku earthquake and tsunami in Japan, a Conference is planned. It will review the lessons learned, the progress made, the things still to be accomplished, and priorities needed for tsunami and similar hazards mitigation. An open house and tour of the Pacific Tsunami Warning Center on Oahu will be available.

Simultaneously, a grand opening of the Hilo Tsunami Museum will take place. The Museum will provide public education programs that will increase tsunami awareness, and will integrate local oral history and scientific information. To achieve its goals, the Museum will have permanent and temporary exhibits, living history talk sessions, and in-house and out-reach education programs. The Museum, a private non-profit organization, welcomes contributions.

The organizing Committee co-Chairmen are George Curtis, Hilo Tsunami Museum, P. O. Box 806, Hilo, Hawaii 96721 and Jim Lander of the University of Colorado.

THE TSUNAMI SOCIETY

SCIENCE OF TSUNAMI HAZARDS

Publication Format for Camera-Ready Copy and Information for Authors:

1. Typing area shown by border.

2. One-column text.

3 All text must be typed single-space. Indent 5 spaces to start a new paragraph.

4. Page numbers in lower right hand corner in pencil or blue marker.

5. Top half of first page to contain the title in capitals, followed by the authors and author affiliation, centered on page.

6. Bottom half of first page to contain the abstract with the heading ABSTRACT centered on page.

Send original and a copy

Dr. Charles Mader, Editor
Mader Consulting Co.
1049 Kamehame Dr., Honolulu, HI. 96825-2860. USA

10" or 25 cm

7½" or 19 cm

APPLICATION FOR MEMBERSHIP

THE TSUNAMI SOCIETY
P. O. Box 25218
Honolulu, Hawaii 96825, USA

I desire admission into the Tsunami Society as: (Check appropriate box.)

☐ Student ☐ Member ☐ Institutional Member

Name _____ Signature _____

Address _____ Phone No. _____

_____

Zip Code _____ Country _____

Employed by _____

Address _____

Title of your position _____

FEE: Student $5.00 Member $25.00 Institution $100.00

Fee includes a subscription to the society journal: SCIENCE OF TSUNAMI HAZARDS.

Send dues for one year with application. Membership shall date from 1 January of the year in which the applicant joins. Membership of an applicant applying on or after October 1 will begin with 1 January of the succeeding calendar year and his first dues payment will be applied to that year.